Received: 14 April 2023 | Accepted: 6 November 2023

DOI: 10.1002/jev2.12381

RESEARCH ARTICLE

Proteome and immune responses of extracellular vesicles derived from macrophages infected with the periodontal pathogen *Tannerella forsythia*

Younggap Lim[1] | **Hyun Young Kim**[1,2] | **Dohyun Han**[3,4,5] | **Bong-Kyu Choi**[1]

[1]Department of Oral Microbiology and Immunology, School of Dentistry, Seoul National University, Seoul, Republic of Korea

[2]Dental Research Institute, School of Dentistry, Seoul National University, Seoul, Republic of Korea

[3]Transdisciplinary Department of Medicine & Advanced Technology, Seoul National University Hospital, Seoul, Republic of Korea

[4]Proteomics Core Facility, Biomedical Research Institute, Seoul National University Hospital, Seoul, Republic of Korea

[5]Department of Medicine, Seoul National University College of Medicine, Seoul, Republic of Korea

Correspondence
Bong-Kyu Choi, Department of Oral Microbiology and Immunology, School of Dentistry, Seoul National University, 101 Daehak-ro, Jongno-gu, Seoul 03080, Republic of Korea.
Email: bongchoi@snu.ac.kr

Dohyun Han, Transdisciplinary Department of Medicine & Advanced Technology, Seoul National University Hospital, 101 Daehak-ro, Jongno-gu, Seoul 03080, Republic of Korea.
Email: hdh03@snu.ac.kr

Funding information
National Research Foundation of Korea, Grant/Award Numbers: NRF-2020R1A5A1019023, NRF-2021R1A2C1003952, NRF-2022R1C1C2007752; Dental Research Institute of Seoul National University; SNUH Research Fund, Grant/Award Number: 2620210020

Abstract

Periodontitis is a chronic inflammatory disease caused by periodontal pathogens in subgingival plaque and is associated with systemic inflammatory diseases. Extracellular vesicles (EVs) released from host cells and pathogens carry a variety of biological molecules and are of interest for their role in disease progression and as diagnostic markers. In the present study, we analysed the proteome and inflammatory response of EVs derived from macrophages infected with *Tannerella forsythia*, a periodontal pathogen. The EVs isolated from the cell conditioned medium of *T. forsythia*-infected macrophages were divided into two distinct vesicles, macrophage-derived EVs and *T. forsythia*-derived OMVs, by size exclusion chromatography combined with density gradient ultracentrifugation. Proteome analysis showed that in *T. forsythia* infection, macrophage-derived EVs were enriched with pro-inflammatory cytokines and inflammatory mediators associated with periodontitis progression. *T. forsythia*-derived OMVs harboured several known virulence factors, including BspA, sialidase, GroEL and various bacterial lipoproteins. *T. forsythia*-derived OMVs induced pro-inflammatory responses via TLR2 activation. In addition, we demonstrated that *T. forsythia* actively released OMVs when *T. forsythia* encountered macrophage-derived soluble molecules. Taken together, our results provide insight into the characterisation of EVs derived from cells infected with a periodontal pathogen.

KEYWORDS
extracellular vesicles, macrophages, periodontitis, proteome, *Tannerella forsythia*

1 | INTRODUCTION

Periodontitis is a chronic inflammatory disease of the tooth-supporting tissue consisting of the gingiva, cementum, periodontal ligament and alveolar bone (Kinane et al., 2017), often leading to alveolar bone resorption and tooth loss (Hajishengallis, 2015). Periodontitis affects approximately 20%–50% of the adult population worldwide and is closely associated with systemic diseases such as Alzheimer's disease, adverse pregnancy outcomes, rheumatoid arthritis, cardiovascular disease and diabetes (Bui et al., 2019; Nazir, 2017).

Extracellular vesicles (EVs) are nanosized vesicles released from living cells that carry various biological cargoes, such as proteins, lipids, nucleic acids and metabolites (Thery et al., 2018). EVs represent the physiological status of donor cells and affect the physiology of recipient cells (Kuipers et al., 2018; Thery et al., 2009). EVs are attracting attention as a valuable tool for disease diagnosis and therapy because EVs play a crucial role in the pathogenesis of diseases and the regeneration of injured tissues (Karn et al., 2021; Sahoo et al., 2021). For instance, macrophages, which are immune cells that sense pathogen invasion and initiate innate immune responses by releasing various inflammatory mediators. EVs derived from macrophages infected with pathogens may carry immunostimulatory molecules that induce inflammatory responses in recipient cells (Arteaga-Blanco & Bou-Habib, 2021). In addition, bacterial EVs can cause systemic inflammatory responses because bacterial EVs easily spread throughout host tissues through the bloodstream and carry bacterial virulence factors (Bittel et al., 2021; Villard et al., 2021). There is growing evidence that EVs derived from periodontal pathogens are associated with atherosclerosis, Alzheimer's disease, rheumatoid arthritis, systemic bone loss and diabetes (Kim et al., 2021; Nara et al., 2021; Okamura et al., 2021; Zhang et al., 2020). However, there is no information on the proteome profiles and immunostimulatory activity of EVs derived from host cells infected with periodontal pathogens.

Tannerella forsythia is a gram-negative anaerobic bacterium isolated from the human gingival pocket of chronic periodontitis patients and is highly associated with the pathogenesis of periodontitis (Sharma, 2010). *T. forsythia* virulence factors such as trypsin-like protease, PrtH protease, sialidase SiaH and NanH, and leucine-rich repeat family BspA allow the bacterium to utilise available nutrients and survive within the host tissue (Chukkapalli et al., 2015; Sharma, 2010). Similar to *T. forsythia* whole cells, *T. forsythia* outer membrane vesicles (OMVs) can stimulate host cells via pattern recognition receptors (PRRs) because *T. forsythia* OMVs harbour virulence factors such as bacterial lipoproteins, glycosylated proteins and BspA (Cecil et al., 2016; Friedrich et al., 2015; Veith et al., 2015).

In the present study, we hypothesised that EVs derived from *T. forsythia*-infected macrophages carry inflammatory mediators of the macrophages and virulence factors of *T. forsythia*, which may affect the pathogenesis of periodontitis and periodontitis-related systemic diseases. We performed in-depth quantitative proteomics and analysed the immune responses to EVs isolated from the cell conditioned medium (CM) of *T. forsythia*-infected human macrophages. The EVs were divided into macrophage-derived EVs and *T. forsythia*-derived OMVs. The macrophage-derived EVs harboured increased levels of pro-inflammatory cytokines and inflammatory mediators. These EVs increased expression of TNF-α in the THP-1 macrophages. The *T. forsythia*-derived OMVs induced the expression of pro-inflammatory cytokines in THP-1 macrophages via TLR2 activation. These results demonstrate that in pathogen-infected cells, EVs derived from host cells and a pathogen can have a synergistic effect on the inflammatory response.

2 | MATERIALS AND METHODS

2.1 | Cells

The THP-1 cells (ATCC TIB-202), a human monocytic cell line, were cultured in an RPMI 1640 medium (Welgene, Daegu, South Korea) supplemented with 10% heat-inactivated foetal bovine serum (FBS; HyClone Laboratories, Inc., Logan, UT), 100 U/mL penicillin and 100 μg/mL streptomycin (Gibco, Waltham, MA) under a humidified 5% CO_2 atmosphere at 37°C. The THP-1 macrophages were prepared as previously described (Jun et al., 2012). The THP-1 cells were differentiated into macrophages by treatment with 500 nM phorbol 12-myristate 13-acetate (PMA; Sigma–Aldrich, St. Louis, MO) for 3 h, washed with sterile PBS (Welgene) and then incubated overnight without PMA. The THP-1 cells were routinely confirmed to be free of mycoplasma contamination using the e-Myco™ plus[2] Mycoplasma PCR Kit (iNtRON Biotechnology, Seongnam, Korea).

To analyze TLR2-mediated cytokine secretion, THP1-Dual™ and THP1-Dual™ KO-TLR2 cells (InvivoGen, San Diego, CA) were used. For cell maintenance, 100 μg/mL Normocin™ (InvivoGen), 10 μg/mL blasticidin (InvivoGen) and 100 μg/mL Zeocin™ (InvivoGen) were added to the culture media according to the manufacturer's instructions.

2.2 | Bacteria culture

Tannerella forsythia ATCC 43037 was cultured in New Oral Spirochete broth (NOS; ATCC medium 1494) supplemented with 10 μg/mL *N*-acetylmuramic acid (NAM; Sigma–Aldrich), 5 μg/mL hemin (Sigma–Aldrich) and 1 μg/mL vitamin K_3 (menadione; Sigma–Aldrich) under anaerobic conditions (10% CO_2, 10% H_2 and 80% N_2) as previously reported (Ko et al., 2019).

To prepare heat-killed *T. forsythia*, the late exponential phase *T. forsythia* was harvested by centrifugation (10,000 × *g*, 10 min, 4°C) and washed with sterile PBS twice. The PBS-resuspended *T. forsythia* was heated at 70°C for 2 h. Heat-killed *T. forsythia* was harvested by centrifugation (10,000 × *g*, 10 min, 4°C) and resuspended in RPMI1640 media (without FBS, penicillin and streptomycin). Complete killing of *T. forsythia* was confirmed by culturing it in NOS broth at 37°C for 3 days.

2.3 | Isolation of crude EVs

The THP-1 macrophages (5×10^7 cells/dish, 150 mm culture dish) were washed three times with sterile PBS and then incubated in RPMI 1640 without FBS, penicillin and streptomycin. A multiplicity of infection (MOI) 50 was used to infect the THP-1 macrophages with *T. forsythia*. The conditioned medium (CM) of the *T. forsythia*-infected THP-1 macrophages was harvested 48 h post-infection. The dead cells, cell debris and large particles in the CM were removed by differential centrifugation at 300 × *g* for 10 min at 4°C, 2000 × *g* for 10 min at 4°C and followed by 10,000 × *g* for 30 min at 4°C, respectively. Then, the centrifuged CM was filtered through a 0.22 μm pore polyethersulfone (PES) membrane filter system (Corning, New York, NY). The clarified CM was concentrated by a 100 kDa molecular weight cutoff (MWCO) centrifugal filter (Centricon®; Merck Millipore, Burlington, MA). The crude EVs were isolated from the concentrated CM by qEV® size exclusion chromatography (Izon Science, Christchurch, New Zealand) according to the manufacturer's instructions. Briefly, 0.5 mL of the concentrated CM was loaded onto the qEV® column, and then 0.5 mL of each fraction was harvested. The concentration of the nanoparticles in each fraction was analyzed by nanoparticle tracking analysis (NTA). The nanoparticle-enriched fractions (routinely fractions #7 to #11) were combined and named crude EVs. The protein concentration of the crude EVs was analysed by a Pierce™ BCA Protein Assay Kit (Thermo Fisher Scientific, Waltham, MA) according to the manufacturer's instructions. For further experiments, the crude EVs were concentrated using a 10 kDa MWCO centrifugal filter (Amicon®; Merck Millipore). For this study, the crude EVs were harvested at least 6 times from 180 mL of the CM from both the non-infected and the *T. forsythia*-infected THP-1 macrophages.

2.4 | Separation of the crude EVs by density gradient ultracentrifugation (DGUC)

The whole crude EVs (1.82×10^{11} particles for the non-infected and 4.36×10^{11} particles for the *T. forsythia*-infected one) were mixed with a 60% iodixanol solution (OptiPrep™; Sigma-Aldrich) to make a 40% iodixanol solution (3.5 mL) and then placed at the bottom of an ultracentrifuge tube. Sterile PBS was mixed with a 60% iodixanol solution to make 35% (1.3 mL), 30% (2.4 mL), 25% (1.5 mL), 20% (2.8 mL) and 5% (1.5 mL) iodixanol solutions. The diluted iodixanol solutions were overlaid on top of the 40% iodixanol-crude EVs to make a discontinuous density gradient. The gradient samples were centrifuged at 100,000 × *g* for 18 h at 4°C using Optima XE-100 (Beckman Coulter, Brea, CA) with a SW40Ti swing bucket rotor (Beckman Coulter). After ultracentrifugation, an equal volume (1.3 mL) of each fraction was harvested from the top of the gradient samples. NTA was used to analyse the nanoparticle concentration of each fraction. To remove the iodixanol, the nanoparticle-enriched fractions were diluted with sterile PBS, ultracentrifuged at 120,000 × *g* for 2 h at 4°C using SW40Ti swing bucket rotor, and the supernatant was discarded. The pellet was resuspended in sterile PBS and stored at −80°C until use.

2.5 | Trypsin treatment of the crude EVs

To analyze real-vesicular proteins, crude EVs were treated with trypsin as previously reported with some modifications (Fitzgerald et al., 2018; Choi et al., 2020). Half of the crude EVs (2.18×10^{11} particles) isolated from the *T. forsythia*-infected THP-1 macrophages were treated with 0.25% trypsin (Gibco) for 30 min at 37°C. For the control, the other half of the crude EVs were treated with equivalent volume of 146 mM NaCl (same media formulation as trypsin). To terminate trypsinisation, a soybean trypsin inhibitor (Gibco) was added to the trypsinised crude EVs. The trypsinised crude EVs were mixed with a 60% iodixanol solution to make a 40% iodixanol solution and set at the bottom of an ultracentrifuge tube, and then density gradient ultracentrifugation was performed as described above.

2.6 | Nanoparticle tracking analysis (NTA)

NanoSight LM10 (Malvern Instruments Ltd., Worcestershire, UK) was used to analyse the size and concentration of the nanoparticles in the samples. Each sample was diluted in nanoparticle-free PBS to adjust the proper concentration range. NTA software (Ver. 2.5, Malvern Instruments Ltd.) was used for data analysis, and the acquisition settings used in this experiment were as follows: screen gain, 12; camera level, 15; and detection threshold, 3.

2.7 | Immunoblotting

The EV samples were directly mixed with a 5X sample buffer (1 M Tris-HCl, pH 6.8, 50% glycerol, 10% sodium dodecyl sulfate (SDS), 5% 2-mercaptoethanol and 0.1% bromophenol blue) and then boiled at 95°C for 10 min. The samples were subjected

to sodium dodecyl sulphate–polyacrylamide gel electrophoresis (SDS-PAGE) and then transferred to polyvinylidene difluoride (PVDF) membranes (Merck Millipore), followed by blocking with 5% nonfat dry milk (Cell Signaling Technology, Danvers, MA) in Tris-buffered saline with 0.1% of Tween 20 (TBST) for 1 h at room temperature (RT). The blocked membranes were incubated with primary antibodies overnight at 4°C. The membranes were washed with TBST three times each for 10 min, followed by incubation with horseradish peroxidase-conjugated secondary antibodies (R&D Systems, Minneapolis, MN) for 1 h at RT. After washing with TBST three times for 10 min each, the membranes were soaked with an ECL solution (Dyne Bio, Seongnam, South Korea) and detected using ChemiDOC (Bio-Rad, Hercules, CA). The primary antibodies used in this study were as follows: anti-CD63 (ab134045, Abcam, Cambridge, UK), anti-CD9 (ab92726, Abcam), anti-Alix (#2171, Cell Signaling Technology), anti-β-actin (#612656, BD Bioscience, San Jose, CA), anti-fibronectin (F3648, Sigma-Aldrich), anti-Histone H3 (#9715, Cell Signaling Technology) and anti-*T. forsythia* (D377-3, MBL, Nagoya, Japan).

2.8 | SYPRO Ruby protein staining

The EV samples were directly mixed with a 5X sample buffer and then boiled at 95°C for 10 min. The samples were subjected to SDS-PAGE, and a gel was stained with SYPRO-Ruby protein gel staining solution (Invitrogen, Waltham, MA) according to the manufacturer's instructions. Briefly, a gel was fixed in 100 mL of fixation solution (50% methanol, 7% acetic acid and 43% deionised water) two times each for 30 min at RT. The fixed gel was stained overnight in 60 mL of SYPRO Ruby protein gel staining solution at RT. The stained gel was washed once with 100 mL of washing buffer (10% methanol, 7% acetic acid and 83% deionised water) for 30 min and then washed twice with 100 mL of deionised water for 5 min. The gel was imaged by ChemiDOC (Bio-Rad).

2.9 | Transmission electron microscopy (TEM)

Five microliters of each EV sample were loaded onto a glow-discharged formvar/carbon-coated copper grid (Electron Microscopy Sciences, Hatfield, PA) for 1 min, washed twice with distilled water, and then stained with 2% uranyl acetate for 1 min. The negatively stained EV samples were imaged by TEM (LIBRA 120; Carl Zeiss, Jena, Germany) at 120 kV.

2.10 | Enzyme-linked immunosorbent assay (ELISA)

The THP-1 macrophages (1×10^5 cells/well) were treated with 1×10^9 particles/mL EVs in a 96-well culture plate. The protein expression levels of TNF-α, IL-1β, IL-6 and IL-8 in the culture supernatants were measured using an ELISA kit (R&D Systems) according to the manufacturer's instructions. The optical density of each well was measured by an Epoch2 Microplate Reader (BioTek Instruments Inc., Winooski, VT) at wavelengths of 450 and 540 nm.

2.11 | Strength measurement of the TLR2 and TLR4 signalling pathway activation

The CHO/CD14/TLR2 and CHO/CD14/TLR4 reporter cells were obtained from Douglas Golenbock (Boston Medical Center, Boston, MA). The strength of the TLR2 or TLR4 signalling pathway activation was measured as previously reported (Kim et al., 2021). Briefly, the CHO/CD14/TLR2 or CHO/CD14/TLR4 cells (3×10^5 cells/well) were seeded on 48-well culture plates in the presence of G418 (1 mg/mL, InvivoGen) and hygromycin B (0.4 mg/mL, InvivoGen) for 20 h in Ham's F-12 Nutrient complete medium (10% FBS, 100 U/mL penicillin and 100 μg/mL streptomycin). Then, the cells were stimulated with the indicated EVs (1×10^9 particles/mL) for 16 h. Pam3CSK4 (100 ng/mL, InvivoGen) and ultrapure LPS (100 ng/mL, InvivoGen) were used as the positive controls for TLR2 and TLR4, respectively. After that, the cells were stained with fluorescein isothiocyanate (FITC) anti-human CD25 antibody (BD Biosciences). The expression of CD25 was analysed by measuring the FITC fluorescence intensity of the cells using a FACS LSRFortessa X-20 (BD Biosciences). The FCS data files were analysed using FlowJo software version 10.1 (BD Biosciences).

2.12 | EV sample preparation for proteome analysis

The EVs in each DGUC fraction were precipitated by 10% trichloroacetic acid (TCA). For EV protein digestion, the EV pellet was reconstituted in 50 μL of SDT buffer [2% SDS, 0.1 M dithiothreitol (DTT) in 0.1 M Tris HCl, pH 8.0]. After being heated at 95°C, the denatured proteins were digested by a filter-aided sample preparation (FASP) method as previously described (Suh et al., 2022) with some modifications. Briefly, the protein samples were loaded onto a 30 kDa MWCO centrifugal filter (Amicon®;

Merck Millipore), and the buffer was exchanged with a UA solution (8 M Urea in 0.1 M Tris-HCl, pH 8.5) via centrifugation. After three buffer exchanges with the UA solution, the reduced cysteines were alkylated with 0.05 M iodoacetamide (IAA) in the UA solution for 30 min at RT in the dark. Thereafter, the UA buffer was exchanged for 40 mM ammonium bicarbonate (ABC) twice. The protein samples were digested with trypsin/LysC (enzyme to substrate ratio of 1:100) at 37°C for 16 h. The resulting peptides were collected in new microcentrifuge tubes via centrifugation, and an additional elution step was performed using 40 mM ABC and 0.5 M NaCl. All resulting peptides were acidified with 10% trifluoroacetic acid and desalted using homemade C18-StageTips as described (Suh et al., 2022). The desalted peptides were completely dried with a vacuum dryer and stored at −80°C.

2.13 | Liquid chromatography—mass spectrometry analysis

The liquid chromatography—mass spectrometry (LC-MS/MS) analysis methods was performed using Quadrupole Orbitrap mass spectrometers, Q-exactive plus (Thermo Fisher Scientific) coupled to an Ultimate 3000 RSLC system (Dionex, Sunnyvale, CA, USA) with a nanoelectrospray source as previously described with some modifications (Suh et al., 2022). The peptide samples were separated on the 2-column setup with a trap column (75 µm I.D. × 2 cm, C18 3 µm, 100 Å) and analytical column (75 µm I.D. × 50 cm, C18 1.9 µm, 100 Å). Before sample injection, the dried peptide samples were redissolved in solvent A (2% acetonitrile and 0.1% formic acid). After the samples were loaded onto the nano-LC, a 180-min gradient from 8% to 30% solvent B (100% acetonitrile and 0.1% formic acid) was applied to all the samples. The spray voltage was 2.0 kV in positive ion mode and the temperature of the heated capillary was set to 320°C. Mass spectra were acquired in data-dependent mode using a top 15 method on a Q Exactive. The Orbitrap analyzer scanned precursor ions with a mass range of 350−1800 m/z and a resolution of 70,000 at m/z 200. Higher-energy collisional dissociation (HCD) scans were acquired on the Q Exactive at a resolution of 35,000. HCD peptide fragments were acquired at a normalised collision energy of 28. The maximum ion injection times for the survey and MS/MS scans were 20 and 80 ms, respectively.

2.14 | Data processing for label-free quantification

Mass spectra were processed with MaxQuant (version 1.6.1.0) (Cox & Mann, 2008). MS/MS spectra were searched against the Human UniProt protein sequence database (October 2020, reviewed, 20,319 entries) and the NCBI RefSeq *T. forsythia* protein sequence database (GCF_006385365.1_ASM638536v1_protein.fasta) using the Andromeda search engine (Cox et al., 2011). Primary searches were performed using a 6 ppm precursor ion tolerance for the analysis of the total protein level. The MS/MS ion tolerance was set to 20 ppm. Cysteine carbamido-methylation was set as a fixed modification. N-terminal acetylation of the proteins and oxidation of methionine were set as variable modifications. Enzyme specificity was set to full tryptic digestion. The peptides with a minimum length of six amino acids and up to two missed cleavages were considered. The required false discovery rate (FDR) was set to 1% at the peptide, protein and modification levels. To maximise the number of quantification events across samples, matching between runs was performed. The mass spectrometry proteomics data have been deposited to the ProteomeXchange Consortium via the PRIDE (Perez-Riverol et al., 2022) partner repository with the dataset identifier PXD047059.

2.15 | Statistical analysis of the proteomic data

Statistical analyses for the proteomic data were performed using Perseus software (Tyanova et al., 2016). Initially, the proteins identified as only identified by site, reverse and contaminants were removed. The expression level of the proteins in each fraction was estimated by determining their intensity-based absolute quantification (iBAQ) values calculated using MaxQuant software. Because of the skewed distribution of the data, log2 transformation was conducted for these values. The valid values were filtered for proteins with a minimum of 70% quantified values in at least one diagnostic group. Missing values were imputed based on a normal distribution (width = 0.3, down-shift = 1.8) to simulate signals of low-abundance proteins. Two-sided *t*-tests were performed for pairwise comparison of the proteomes to detect differentially expressed proteins (DEPs). The protein abundances were subjected to *z*-normalisation followed by hierarchical clustering with Pearson's correlation distance.

2.16 | Bioinformatics analysis

The disease and Gene Ontology biological process (GOBP) enrichment analysis of differentially expressed human proteins in NI-F2 and TF-F2 was conducted using the Database for Annotation, Visualisation and Integrated Discovery (DAVID) (https://david.ncifcrf.gov/home.jsp) and the ShinyGO (v0.77) bioinformatics tool (http://bioinformatics.sdstate.edu/go/), respectively (Ge et al., 2020). Gene Ontology cellular component (GOCC) enrichment analysis of human proteins identified in NI-F2 and

TF-F2 was performed using the DAVID based on Gene Ontology (GO) annotations (GOCC and GOCC_DIRECT). The subcellular localisation of human proteins identified in NI-F2 and TF-F2 was predicted using protein sequences based on protein language models and deep learning (DeepLoc v2.0, https://services.healthtech.dtu.dk/services/DeepLoc-2.0/) (Thumuluri et al., 2022). The subcellular localisation of *T. forsythia* proteins was analysed by CELLO v2.5 (http://cello.life.nctu.edu.tw/) from the Molecular Bioinformatics Center of National Chiao Tung University (Yu et al., 2014). The lipid attachment site of each *T. forsythia* protein was predicted by the ExPASy-PROSITE protein domain database (https://prosite.expasy.org/). *T. forsythia* proteins were categorised into their functions according to their domains described in the GenBank database of the National Center for Biotechnology Information (NCBI).

2.17 | Culture of the live *T. forsythia* in the EV-free conditioned medium of the THP-1 macrophages

The THP-1 macrophages (5×10^7 cells/dish) were infected with the MOI 50 of *T. forsythia* and cultured in RPMI 1640 without FBS supplementation for 24 h under a humidified 5% CO_2 atmosphere at 37°C. The CM was harvested and clarified by differential centrifugation at 300 × *g* for 10 min at 4°C, 2000 × *g* for 10 min at 4°C, and 10,000 × *g* for 30 min at 4°C. Biomolecules over 100 kDa, non-vesicular aggregates, and EVs in the clarified CM were eliminated by 100 kDa MWCO ultrafiltration. The filtrate was confirmed to be free of nanoparticles by NTA. The filtrate was treated with live *T. forsythia* in 150 mm cell culture dishes for 24 h under a humidified 5% CO_2 atmosphere at 37°C. The *T. forsythia* CM was harvested and centrifuged at 10,000 × *g* for 10 min at 4°C, and then the pellet was discarded. As described above, the EVs in the *T. forsythia* CM were isolated by size exclusion chromatography combined with DGUC.

2.18 | Statistics

The mean value ± standard deviation was determined for each group. One-way analysis of variance (ANOVA) with Dunnett's post-test was used to determine the significance of differences among more than two groups. Two-way ANOVA with Sidak's post-test was used to examine the difference between two categorical independent variables. A *p*-value less than 0.05 was considered statistically significant. All statistical analyses were performed using GraphPad Prism software (GraphPad Software Inc., San Diego, CA).

3 | RESULTS

3.1 | Two distinct types of EVs were isolated from the conditioned medium of *T. forsythia*-infected macrophages

EVs were isolated from the CM of *T. forsythia*-infected macrophages by size exclusion chromatography combined with DGUC (Figure 1a). As a control, additional EVs were isolated from the CM of non-infected macrophages and analysed simultaneously with the EVs derived from the infected macrophages. Approximately, $1.82 \times 10^{11} \pm 5.02 \times 10^{10}$ particles (as protein, 98.4 ± 18.2 μg) of the crude EVs were isolated from the non-infected THP-1 macrophages and $4.36 \times 10^{11} \pm 1.33 \times 10^{11}$ particles (as protein, 265.3 ± 97.1 μg) of the crude EVs were isolated from the *T. forsythia*-infected THP-1 macrophages. The viability was 93.01 ± 2.63% for non-infected THP-1 macrophages and 89.81 ± 1.43% for *T. forsythia*-infected THP-1 macrophages, at the point of EV isolation (Figure S1).

The density gradient fractions were divided into 10 fractions (NI-F1 to NI-F10 for the non-infected cells and TF-F1 to TF-F10 for the *T. forsythia*-infected cells). The nanoparticles were enriched in NI-F2 and NI-F3, while few nanoparticles were observed in the other fractions (Figure 1b). The protein profiles of NI-F2 and NI-F3 were completely different from those of the NI-F5 to NI-F10 fractions (Figure 1c). TEM images showed that EVs were detected in NI-F2 (Figure 1d), whereas there were only small non-vesicular aggregates in NI-F5 and NI-F7. The markers of mammalian EVs, such as CD9 and CD63, were enriched in NI-F2 and NI-F3 (Figure 1e). However, host proteins such as fibronectin and histone H3, known as non-vesicular aggregates proteins (Jeppesen et al., 2019), were enriched in NI-F5 to NI-F7. Consistent with previous reports, β-actin was identified in all the fractions except for NI-F1, indicating the presence of both vesicular and non-vesicular forms (Jeppesen et al., 2019).

Unlike the EVs derived from the CM of non-infected macrophages, the nanoparticles derived from the CM of *T. forsythia*-infected macrophages were divided into three parts by DGUC (Figure 1b,c). TEM images showed that the EVs were detected in not only TF-F2 but also TF-F5, while the non-vesicular aggregates, similar in size to the EVs, were observed in TF-F7 (Figure 1d). The expression patterns of the mammalian EV markers (CD9 and CD63) and non-vesicular proteins (fibronectin and histone H3) were similar to those of the non-infected EVs (Figure 1e). Furthermore, the *T. forsythia* proteins were highly enriched in TF-F4 to TF-F6 (Figure 1e). These results demonstrate that host cell-derived EVs and bacteria-derived OMVs coexist at different densities during *T. forsythia* infection.

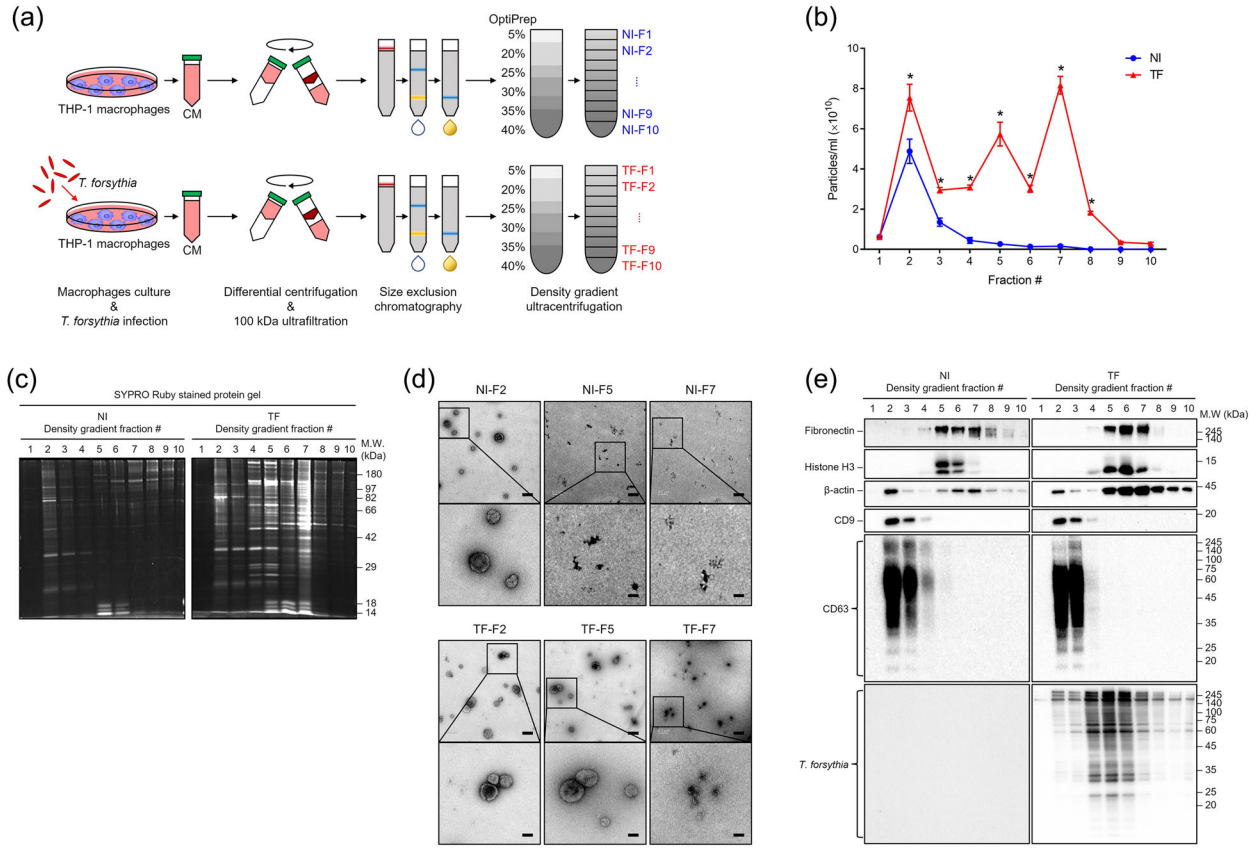

FIGURE 1 Characterisation of the two distinct types of EVs derived from the CM of macrophages infected with *T. forsythia*. (a) Schematic diagram of the EV isolation procedure. (b) The nanoparticle concentration in each density gradient fraction was analysed by NTA. (c) Each density gradient fraction was subjected to SDS-PAGE and stained with SYPRO Ruby protein gel staining solution. The fluorescence of the protein bands was imaged by a UV transilluminator. (d) The indicated fractions were negatively stained and imaged by TEM. Scale bar: 200 nm for wide-field images and 50 nm for close-up images. (e) Density gradient fractions were analysed by immunoblotting using the indicated antibodies. The experiments were performed at least three times independently. The data are presented as the mean ± standard deviation of triplicate assays and were analysed by two-way ANOVA. NI, Non-infection group; TF, *T. forsythia* infection group. $^*p < 0.05$.

Next, to analyse whether mammalian EV markers and *T. forsythia* proteins are real-vesicular proteins, the EVs and OMVs derived from the CM of *T. forsythia*-infected macrophages were treated with trypsin and then subjected to DGUC (Figure 2). Trypsin treatment to EVs is useful method to analyse real-vesicular proteins since trypsin could not penetrate the lipid-bilayer of the EVs and only eliminate proteins outside of the EVs (Choi et al., 2020; Fitzgerald et al., 2018). Trypsinisation barely affected the particle concentration, protein profile and morphology of the EVs in TF-F2 and TF-F5 when analysed by NTA, SDS-PAGE and TEM (Figure 2a–c). However, the particle concentration and proteins in TF-F7 were significantly reduced by trypsin treatment (Figure 2a,b). In F7–F10, the distinct bands around 16 and 20 kDa were soybean trypsin inhibitor, and two distinct bands around 25—30 kDa were trypsin (Figure 2b). The mammalian EV markers (Alix and CD63) in TF-F2 and the *T. forsythia* proteins in TF-F5 were not affected by trypsin treatment (Figure 2d). Interestingly, the human proteins (fibronectin, histone H3 and β-actin) in TF-F5 and TF-F7 were eliminated by trypsin treatment (Figure 2d).

These data suggest that first, the EVs in TF-F5 were *T. forsythia*-derived OMVs. Second, the non-vesicular human proteins were more abundant in the higher density fractions (F5 to F7) than the macrophage-derived EVs (F2 to F3). Additionally, it is important to note that enzymatic reactions such as trypsinisation may be necessary to differentiate between non-vesicular and vesicular proteins.

3.2 | The EVs and OMVs derived from the CM of non-infected and *T. forsythia*-infected macrophages were analysed by in-depth quantitative proteomics

The proteomes of the two distinct EVs were analysed by in-depth quantitative proteomics (Figure 3a). The EVs and OMVs of TF-F2 and TF-F5 from the CM of *T. forsythia*-infected macrophages were used for proteome analysis. And the proteome of the

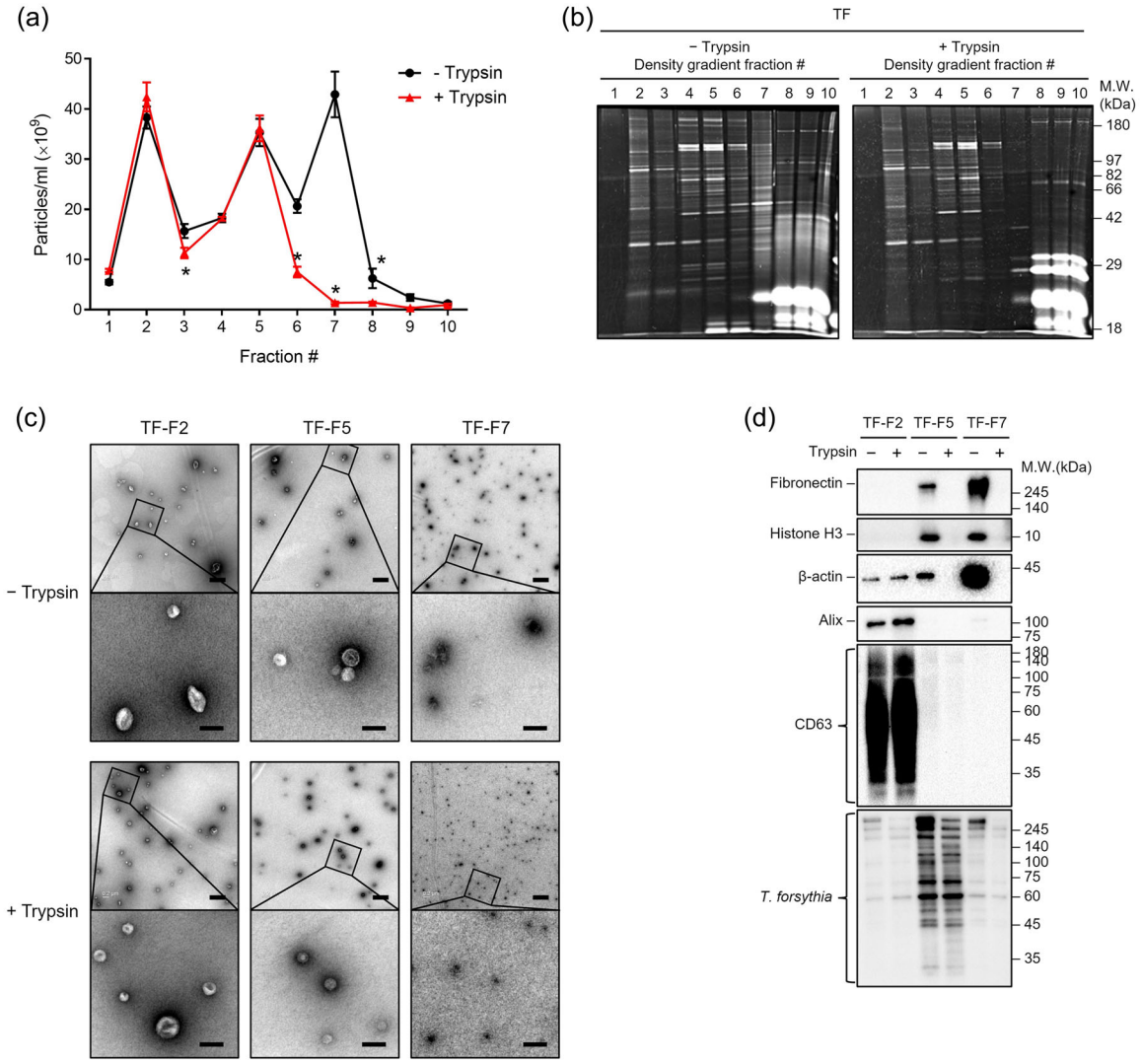

FIGURE 2 Elimination of the non-vesicular proteins by trypsinisation. (a) Nanoparticle concentrations in each density gradient fraction of the *T. forsythia*-infected EVs with or without trypsinisation were analysed by NTA. (b) Each density gradient fraction was subjected to SDS-PAGE and stained with SYPRO Ruby protein gel staining solution. The fluorescence of the protein bands was imaged by a UV transilluminator. (c) The indicated fractions were negatively stained and imaged by TEM. Scale bar: 400 nm for wide-field images and 100 nm for close-up images. (d) The indicated fractions were analysed by immunoblotting using the indicated antibodies. The experiments were performed at least three times independently. The data are presented as the mean ± standard deviation of triplicate assays and were analysed by two-way ANOVA. TF, *T. forsythia* infection group. $^*p < 0.05$.

NI-F2 EVs from the CM of non-infected macrophages was analysed as the control. Even though human proteins were identified in TF-F5, only *T. forsythia* proteins were analysed since they were non-vesicular proteins.

A total of 1596 proteins were identified. There were 1247 human proteins and 349 *T. forsythia* proteins. Principal component analysis (PCA) showed that the proteome compositions were completely different between each treatment group (Figure 3b). DeepLoc was used to predict the subcellular localisation of human proteins in NI-F2 and TF-F2 (Figure S2a, S2b, and Table S1). Thumuluri et al. reported the subcellular localisation of total human proteins using this method (Thumuluri et al., 2022). Human proteins in NI-F2 and TF-F2 were grouped according to Gene Ontology cellular compartment (GOCC) annotations (Figure S2c and Table S1). Human proteins in NI-F2 and TF-F2 were enriched in extracellular region part (GO:0044421) and extracellular region (GO:000455576), especially extracellular exosome (GO:0070062) (Table S1). The differentially expressed human proteins of NI-F2 and TF-F2 are represented by a volcano plot (Figure 3c and Table 1). We conducted disease enrichment analysis using DAVID on the differentially expressed proteins of TF-F2 and NI-F2. In the disease enrichment analysis, the genes associated with periodontitis were identified in TF-F2, including IL1B (P01584), HLA-B (P01889), MMP9 (P14780), SPP1 (P10451) and TNF (P01375) (Table S2, Figure 3c). We also analysed the Gene Ontology (GO) of the differentially expressed proteins in TF-F2 and NI-F2 (Figure 3d). GO biological process (GOBP) showed that proteins related to neutrophil activation (GO:0042119), granulocyte activation (GO:0036230), leukocyte mediated immunity (GO:0002443), export from cell (GO:0140352), secretion

TABLE 1 Identification of the differentially expressed human proteins in NI-F2 and TF-F2.

Uniprot Accession	Protein name	Gene name	−Log10 (*p*-value)	Difference[a]
I. Differentially expressed human proteins in TF-F2				
P01375	Tumour necrosis factor	TNF	7.3	−7.5
P10145	Interleukin-8	CXCL8	7.6	−6.8
P01584	Interleukin-1 beta	IL1B	6.3	−5.6
Q9NUQ9	Protein FAM49B	FAM49B	3.8	−5.5
P01889	HLA class I histocompatibility antigen, B-7 alpha chain	HLA-B	3.2	−5.3
Q8NA29	Sodium-dependent lysophosphatidylcholine symporter 1	MFSD2A	4.3	−5.2
P29966	Myristoylated alanine-rich C-kinase substrate	MARCKS	3.7	−5.1
Q99829	Copine-1	CPNE1	3.1	−4.9
Q9BSA4	Protein tweety homolog 2	TTYH2	3.9	−4.9
Q9NP72	Ras-related protein Rab-18	RAB18	2.8	−4.8
Q16772	Glutathione S-transferase A3	GSTA3	2.2	−4.8
Q9H3Z4	DnaJ homolog subfamily C member 5	DNAJC5	2.1	−4.8
Q9Y3L5	Ras-related protein Rap-2c	RAP2C	2.1	−4.6
P23526	Adenosylhomocysteinase	AHCY	2.7	−4.5
P17987	T-complex protein 1 subunit alpha	TCP1	6.9	−4.4
P10451	Osteopontin	SPP1	2.5	−4.4
O15162	Phospholipid scramblase 1	PLSCR1	2.5	−4.2
Q9UHL4	Dipeptidyl peptidase 2	DPP7	3.8	−4.2
P11766	Alcohol dehydrogenase class-3	ADH5	2.1	−4.0
P12931	Proto-oncogene tyrosine-protein kinase Src	SRC	3.8	−3.9
Q9NPH3	Interleukin-1 receptor accessory protein	IL1RAP	3.3	−3.8
Q99571	P2X purinoceptor 4	P2RX4	2	−3.7
Q9Y5K6	CD2-associated protein	CD2AP	2.2	−3.5
O75558	Syntaxin-11	STX11	3.2	−3.5
P40227	T-complex protein 1 subunit zeta	CCT6A	2	−3.5
P30679	Guanine nucleotide-binding protein subunit alpha-15	GNA15	3.5	−3.4
Q8IVF7	Formin-like protein 3	FMNL3	3.3	−3.3
P14780	Matrix metalloproteinase-9	MMP9	4.7	−3.3
P49591	Serine–tRNA ligase, cytoplasmic	SARS	2.7	−3.2
Q9UBV8	Peflin	PEF1	3	−3.2
P50897	Palmitoyl-protein thioesterase 1	PPT1	2.3	−3.1
P60174	Triosephosphate isomerase	TPI1	3.7	−3.1
Q9Y6W3	Calpain-7	CAPN7	2.4	−3.0
P09972	Fructose-bisphosphate aldolase C	ALDOC	2.2	−2.9
P45880	Voltage-dependent anion-selective channel protein 2	VDAC2	2.8	−2.9
Q15833	Syntaxin-binding protein 2	STXBP2	2	−2.8
P18077	60S ribosomal protein L35a	RPL35A	2.2	−2.7
O95197	Reticulon-3	RTN3	2.9	−2.7
Q02543	60S ribosomal protein L18a	RPL18A	2.1	−2.7

(Continues)

TABLE 1 (Continued)

Uniprot Accession	Protein name	Gene name	−Log10 (*p*-value)	Difference[a]
P14384	Carboxypeptidase M	CPM	5.4	−2.7
P26640	Valine–tRNA ligase	VARS	2.1	−2.7
Q9UBQ0	Vacuolar protein sorting-associated protein 29	VPS29	2.1	−2.6
P49327	Fatty acid synthase	FASN	2.2	−2.4
Q9UIQ6	Leucyl-cystinyl aminopeptidase	LNPEP	2.9	−2.4
Q9NZM1	Myoferlin	MYOF	2.4	−2.4
P13010	X-ray repair cross-complementing protein 5	XRCC5	3	−2.3
Q96D96	Voltage-gated hydrogen channel 1	HVCN1	2.5	−2.3
P20073	Annexin A7	ANXA7	4.2	−2.2
Q969P0	Immunoglobulin superfamily member 8	IGSF8	2.5	−2.2
O00571	ATP-dependent RNA helicase DDX3X	DDX3X	2.3	−2.2
O00754	Lysosomal alpha-mannosidase	MAN2B1	3.8	−2.2
B0I1T2	Unconventional myosin-Ig	MYO1G	2.1	−2.1
O95477	ATP-binding cassette sub-family A member 1	ABCA1	3.9	−2.0
P11586	C-1-tetrahydrofolate synthase, cytoplasmic	MTHFD1	2.2	−2.0
P26196	Probable ATP-dependent RNA helicase DDX6	DDX6	2.5	−1.9
P08133	Annexin A6	ANXA6	2.5	−1.9
O60884	DnaJ homolog subfamily A member 2	DNAJA2	2.2	−1.8
P54709	Sodium/potassium-transporting ATPase subunit beta-3	ATP1B3	2.2	−1.8
Q9UN37	Vacuolar protein sorting-associated protein 4A	VPS4A	2.5	−1.7
P27701	CD82 antigen	CD82	2.3	−1.7
Q14699	Raftlin	RFTN1	3	−1.5
P13796	Plastin-2	LCP1	2.2	−1.3
P50990	T-complex protein 1 subunit theta	CCT8	2.4	−1.2
P05106	Integrin beta-3	ITGB3	2.6	−1.2
P07737	Profilin-1	PFN1	3.6	−1.1
P20020	Plasma membrane calcium-transporting ATPase 1	ATP2B1	4.6	−1.0
Q09666	Neuroblast differentiation-associated protein AHNAK	AHNAK	2.8	−0.9
P0DMV9	Heat shock 70 kDa protein 1B	HSPA1B	2.9	−0.9
Q99961	Endophilin-A2	SH3GL1	2.1	−0.8
II. Differentially expressed human proteins in NI-F2				
Q9Y287	Integral membrane protein 2B	ITM2B	2.2	3.1
P0DOX5	Ig gamma-1 chain C region	IGHG1	2.6	3.1
Q9H223	EH domain-containing protein 4	EHD4	5.6	3
P01876	Ig alpha-1 chain C region	IGHA1	2.2	3
P21580	Tumour necrosis factor alpha-induced protein 3	TNFAIP3	3.8	3

(Continues)

TABLE 1 (Continued)

Uniprot Accession	Protein name	Gene name	−Log10 (*p*-value)	Difference[a]
O60506	Heterogeneous nuclear ribonucleoprotein Q	SYNCRIP	2.4	2.8
P52566	Rho GDP-dissociation inhibitor 2	ARHGDIB	4.8	2.6
P55899	IgG receptor FcRn large subunit p51	FCGRT	2.3	2.5
P31947	14-3-3 protein sigma	SFN	2.4	2.5
P01860	Ig gamma-3 chain C region	IGHG3	2.3	2.5
Q01469	Fatty acid-binding protein, epidermal	FABP5	3	2.5
P81605	Dermcidin;Survival-promoting peptide	DCD	2.6	2.5
Q96L08	Sushi domain-containing protein 3	SUSD3	3.3	2.4
P40121	Macrophage-capping protein	CAPG	2.1	2.3
O43760	Synaptogyrin-2	SYNGR2	2.6	2.3
P00450	Ceruloplasmin	CP	2.1	2.2
O00468	Agrin	AGRN	2.1	2.2
P34741	Syndecan-2	SDC2	3.5	2.2
Q8IV08	Phospholipase D3	PLD3	2.6	2.2
O14745	Na(+)/H(+) exchange regulatory cofactor NHE-RF1	SLC9A3R1	5	2.2
P27348	14-3-3 protein theta	YWHAQ	2.8	2.1
O14672	Disintegrin and metalloproteinase domain-containing protein 10	ADAM10	4.1	2.1
Q71DI3	Histone H3.2	HIST2H3A	2.6	2.1
P61981	14-3-3 protein gamma	YWHAG	2.1	2
Q7Z2W4	Zinc finger CCCH-type antiviral protein 1	ZC3HAV1	2.8	1.9
Q8NBI5	Solute carrier family 43 member 3	SLC43A3	3.1	6.1
P52272	Heterogeneous nuclear ribonucleoprotein M	HNRNPM	3.5	5.4
P01859	Ig gamma-2 chain C region	IGHG2	2.8	4.8
P01009	Alpha-1-antitrypsin	SERPINA1	2.9	4.5
O43914	TYRO protein tyrosine kinase-binding protein	TYROBP	3.7	4.3
P15309	Prostatic acid phosphatase	ACPP	4.3	4.2
P02647	Apolipoprotein A-I	APOA1	3	4.2
P01024	Complement C3	C3	3.3	3.7
P00738	Haptoglobin	HP	3.1	3.6
P0C0L5	Complement C4-B	C4B	5.4	3.5
Q9P0V8	SLAM family member 8	SLAMF8	2	3.5
P02787	Serotransferrin	TF	2.7	3.4
Q9UI08	Ena/VASP-like protein	EVL	2.6	3.4
P15260	Interferon gamma receptor 1	IFNGR1	2.9	3.3
Q9P2B2	Prostaglandin F2 receptor negative regulator	PTGFRN	2.6	1.9
Q96BY6	Dedicator of cytokinesis protein 10	DOCK10	3.9	1.8
O43399	Tumour protein D54	TPD52L2	2.1	1.8
P16150	Leukosialin	SPN	3.8	1.8
P02671	Fibrinogen alpha chain	FGA	2.1	1.7

(Continues)

TABLE 1 (Continued)

Uniprot Accession	Protein name	Gene name	−Log10 (*p*-value)	Difference[a]
Q13571	Lysosomal-associated transmembrane protein 5	LAPTM5	2.1	1.7
P62258	14-3-3 protein epsilon	YWHAE	3.5	1.6
Q96C86	m7GpppX diphosphatase	DCPS	2.2	1.6
P11215	Integrin alpha-M	ITGAM	2.7	1.6
Q99828	Calcium and integrin-binding protein 1	CIB1	3.1	1.6
P20702	Integrin alpha-X	ITGAX	2.9	1.6
P23229	Integrin alpha-6	ITGA6	2.2	1.6
Q86YQ8	Copine-8	CPNE8	4.8	1.6
P05556	Integrin beta-1	ITGB1	2.8	1.5
P19623	Spermidine synthase	SRM	2.3	1.5
P31946	14-3-3 protein beta/alpha	YWHAB	2.3	1.5
P06753	Tropomyosin alpha-3 chain	TPM3	3.9	1.4
P50281	Matrix metalloproteinase-14	MMP14	2.3	1.4
Q96TA1	Niban-like protein 1	FAM129B	5	1.3
O00232	26S proteasome non-ATPase regulatory subunit 12	PSMD12	2.5	1.3
O75044	SLIT-ROBO Rho GTPase-activating protein 2	SRGAP2	3	1.3
Q7L576	Cytoplasmic FMR1-interacting protein 1	CYFIP1	3.2	1.3
P08648	Integrin alpha-5	ITGA5	2.6	1.1
O95819	Mitogen-activated protein kinase kinase kinase kinase 4	MAP4K4	2.8	1.1
P53990	IST1 homolog	IST1	2.3	1.1
Q5TZA2	Rootletin	CROCC	3.5	1.1
O43633	Charged multivesicular body protein 2a	CHMP2A	2.2	1.1
P42356	Phosphatidylinositol 4-kinase alpha	PI4KA	2.6	1.1
P00338	L-lactate dehydrogenase A chain	LDHA	2.7	1
P62834	Ras-related protein Rap-1A	RAP1A	2.3	1
P20701	Integrin alpha-L	ITGAL	2.5	1
P52565	Rho GDP-dissociation inhibitor 1	ARHGDIA	2.1	0.9
P22732	Solute carrier family 2, facilitated glucose transporter member 5	SLC2A5	2.3	0.8
P62993	Growth factor receptor-bound protein 2	GRB2	2.3	0.8
P08582	Melanotransferrin	MFI2	2.4	0.7
Q9ULI3	Protein HEG homolog 1	HEG1	2.6	0.6

[a]Difference: Log2 (Fold-change NI-F2 vs. TF-F2).

by cell (GO:0032940) and secretion (GO:0046903) were enriched in TF-F2, whereas proteins associated with regulation of protein localisation to membrane (GO:1905475), cell morphogenesis involved in differentiation (GO:0000904), leukocyte activation (GO:0045321), cell migration (GO:0016477), cell motility (GO:0048870) and localisation of cell (GO:0051674) were enriched in NI-F2 (Figure 3d). These results indicate that in *T. forsythia* infection, macrophage-derived EVs carry various proteins that are associated with the progression of periodontitis and the activation of immune cells.

The proteome analysis identified 349 *T. forsythia* proteins in TF-F5, of which 170 of the proteins have been identified in previous reports on *T. forsythia* OMVs (Friedrich et al., 2015; Veith et al., 2015) and 179 proteins were identified in this

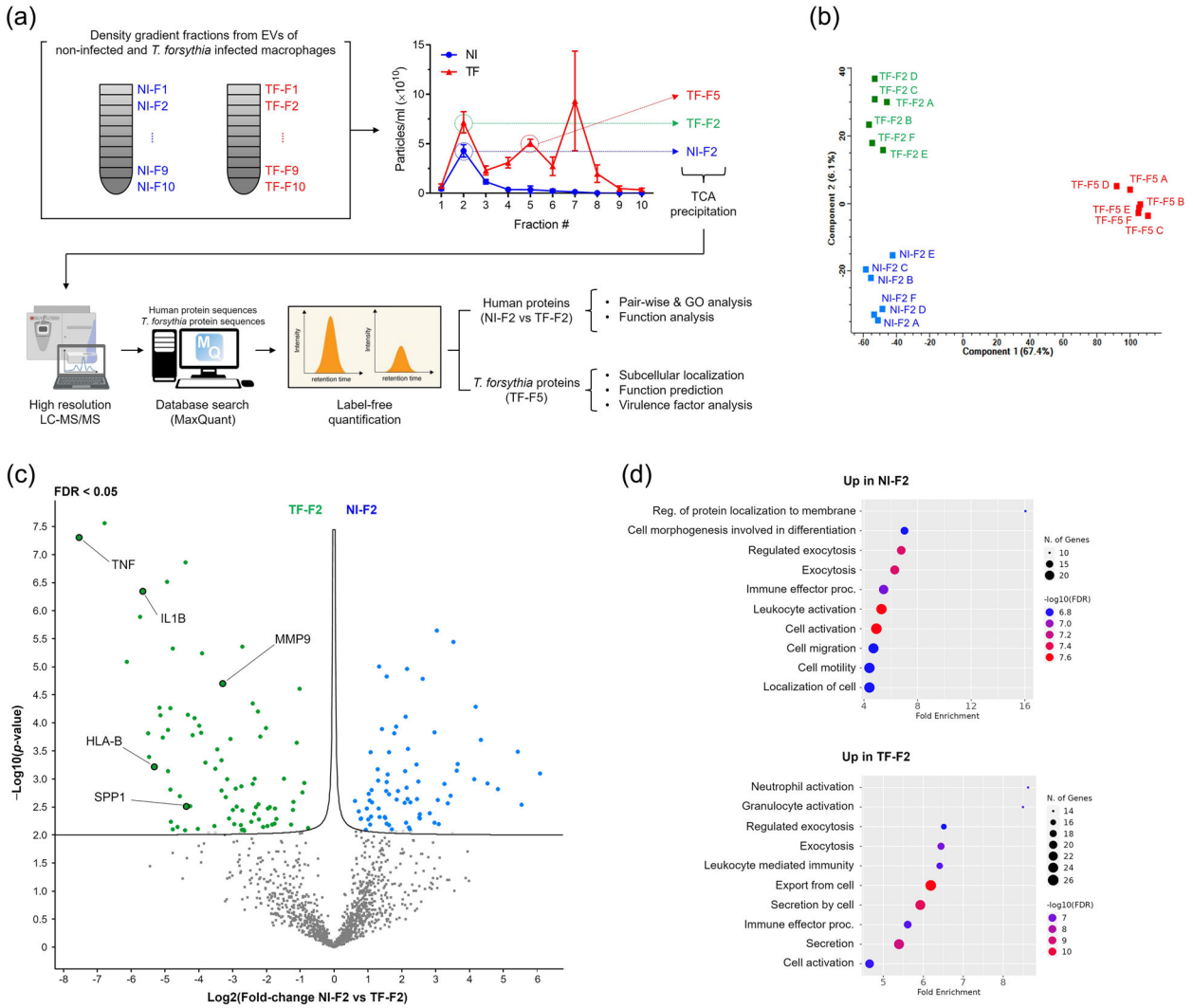

FIGURE 3 In-depth quantitative proteomic analysis of the macrophage-derived EVs from the non-infected and *T. forsythia*-infected macrophages. (a) Diagram representing the in-depth quantitative proteomic analysis of the EVs derived from the non-infected and *T. forsythia*-infected macrophages by the label-free quantification method. The in-depth quantitative proteomic analysis was performed using EV samples from the six independent experiments. Nanoparticle concentrations of six independently performed DGUC samples were analysed by NTA. NI-F2, TF-F2 and TF-F5 were pelleted by TCA precipitation and then analysed by LC-MS/MS. (b) Principal component analysis (PCA) results of the proteome of the three different EVs. (c) Volcano plot depicting the differentially expressed proteins between NI-F2 and TF-F2. The false discovery rate (FDR) was less than 0.05. In the disease enrichment analysis, genes associated with periodontitis were identified and visualised on a volcano plot. (d) GO was analysed for the biological process by ShinyGO. The dot plot shows the top 10 GO terms ranked by fold enrichment. NI, Non-infection group; TF, *T. forsythia* infection group.

study (Table 2). According to Yoo et al., 12 proteins were upregulated by *in vivo*-induced antigen technology (IVIAT) using serum from periodontitis patients (Yoo et al., 2007). Among them, we identified seven proteins in TF-F5, including TonB-dependent receptor plug domain-containing protein (WP_046825933.1), RagB/SusD family nutrient uptake outer membrane protein (WP_046825921.1), two S9 family peptidases (WP_046825437.1 and WP_046824629.1), leucine-rich-repeat family virulence factor BspA (WP_052449061.1), OmpA family protein (WP_046824554.1) and beta-glucosidase BglX (WP_080948511.1). The subcellular localisation of the *T. forsythia* proteins was analysed using the CELLO database: outer membrane proteins accounted for the highest proportion (138 proteins, 39.5%), followed by cytoplasmic (88 proteins, 25.2%), periplasmic (86 proteins, 24.6%), extracellular (32 proteins, 9.2%) and inner membrane proteins (5 proteins, 1.4%) (Table 2, Figure S3). This composition was similar to the previously reported proteome of *T. forsythia* OMVs (Friedrich et al., 2015). A total of 95 bacterial lipoproteins (27.2%) were predicted by the ExPASy-PROSITE protein domain database (Table 2). All the *T. forsythia* proteins were categorised into their functions according to their domains described in the GenBank database. TonB-dependent receptors and their associated proteins occupied the largest portion (96 proteins, 27.5%). Twenty-one proteins (6.0%) were components of the type IX secretion system (T9SS) and its substrates. Thirty-two proteins (9.2%) were peptidases, and 12 proteins (3.4%) were glycosyl hydrolases. Ten proteins (2.9%) were proteins with tetratricopeptide repeat domains. Four proteins (1.1%) were TolC

TABLE 2 Identification and characterisation of the *T. forsythia* proteins in TF-F5.

Accession	Definition	Amino acid	M.W. (kDa)	iBAQ	Previously reported proteins of Tf OMVs	Predicted subsellular location[c]	Lipoprotein[d]
I. TonB-dependent receptors and their associated proteins (96/349)							
i. TonB-dependent receptor plug (55/349)							
WP_046824810.1	TonB-dependent receptor	670	76.2	94140000		Outer Membrane	
WP_046825933.1	TonB-dependent receptor plug domain-containing protein	709	81.3	71073167		Outer membrane	
WP_046824469.1	TonB-dependent receptor	770	87.2	54803500	[a,b]	Outer membrane	
WP_087879765.1	TonB-dependent receptor	780	88.3	40526550		Outer membrane	
WP_161794935.1	TonB-dependent receptor	767	87.4	35777250		Outer membrane	
WP_046825715.1	TonB-dependent receptor	748	84.9	32609000		Outer membrane	
WP_070098097.1	TonB-dependent receptor	852	95.2	27993667		Outer membrane	
WP_046825711.1	TonB-dependent receptor	744	83.5	14834817		Outer membrane	
WP_046826211.1	TonB-dependent receptor	928	104.2	13375917	[a]	Outer membrane	
WP_046826221.1	TonB-dependent receptor	786	89.2	9320383		Outer membrane	
WP_052449006.1	DUF5686 and carboxypeptidase regulatory-like domain-containing protein	897	102.3	9148317		Outer membrane	
WP_046824884.1	TonB-dependent receptor	952	106.7	8590233		Outer membrane	
WP_046824887.1	TonB-dependent receptor	780	87.5	8294233		Outer membrane	
WP_052449124.1	TonB-dependent receptor	983	110.2	7792183		Outer membrane	
WP_014226387.1	TonB-dependent receptor	818	92.2	6380600	[a]	Outer membrane	
WP_046824590.1	carboxypeptidase regulatory-like domain-containing protein	1085	121	6245667	[a,b]	Outer membrane	
WP_004585028.1	MULTISPECIES: carboxypeptidase regulatory-like domain-containing protein	891	100.4	5730183		Outer membrane	
WP_052449117.1	TonB-dependent receptor	1154	129	5536433	[a,b]	Outer membrane	
WP_046824978.1	TonB-dependent receptor	1179	132.7	4487350	[a]	Outer membrane	
WP_052449113.1	TonB-dependent receptor	1148	128.3	4306783		Outer membrane	

(Continues)

TABLE 2 (Continued)

Accession	Definition	Amino acid	M.W. (kDa)	iBAQ	Previously reported proteins of Tf OMVs	Predicted subsellular location[c]	Lipoprotein[d]
WP_161794958.1	SusC/RagA family TonB-linked outer membrane protein	1121	125.2	4070500		Outer membrane	
WP_052449077.1	TonB-dependent receptor	1134	128.3	2995100		Outer membrane	
WP_052449042.1	SusC/RagA family TonB-linked outer membrane protein	1072	119.4	2654435		Outer membrane	
WP_080948581.1	TonB-dependent receptor	1154	128.8	2237838		Outer membrane	
WP_046825765.1	TonB-dependent receptor	1156	130.3	2234495	[a]	Outer membrane	
WP_080948590.1	TonB-dependent receptor	1131	125.4	1920207		Outer membrane	
WP_046825251.1	TonB-dependent receptor	1100	122.4	1670988		Outer membrane	
WP_080948655.1	TonB-dependent receptor	1127	124.6	1556477		Outer membrane	
WP_046825525.1	SusC/RagA family TonB-linked outer membrane protein	1032	113.6	1479112	[a,b]	Outer membrane	
WP_046825920.1	TonB-dependent receptor	1091	121.3	1451193	[a,b]	Outer membrane	
WP_046824947.1	TonB-dependent receptor	1194	133	1236392	[a,b]	Outer membrane	
WP_046825759.1	SusC/RagA family TonB-linked outer membrane protein	1055	116.2	1091712	[a,b]	Outer membrane	
WP_052448943.1	SusC/RagA family TonB-linked outer membrane protein	984	111.4	1028220		Outer membrane	
WP_046825522.1	SusC/RagA family TonB-linked outer membrane protein	1064	117.3	961290	[a,b]	Outer membrane	
WP_041590774.1	TonB-dependent receptor	1096	123	934603	[a]	Outer membrane	
WP_140230659.1	TonB-dependent receptor	1021	113.1	726948		Outer membrane	
WP_080948647.1	TonB-dependent receptor	1049	117.8	681305		Outer membrane	
WP_052449079.1	TonB-dependent receptor	1062	118.4	569730	[a,b]	Outer membrane	
WP_046826204.1	TonB-dependent receptor	1014	112.2	396201	[a,b]	Outer membrane	
WP_052449046.1	TonB-dependent receptor	1013	114	284142		Outer membrane	
WP_046824487.1	TonB-dependent receptor	1009	112.3	283865		Outer membrane	
WP_201774571.1	SusC/RagA family TonB-linked outer membrane protein	1022	111.8	209296		Outer membrane	

(Continues)

TABLE 2 (Continued)

Accession	Definition	Amino acid	M.W. (kDa)	iBAQ	Previously reported proteins of Tf OMVs	Predicted subsellular location[c]	Lipoprotein[d]
WP_046825289.1	SusC/RagA family TonB-linked outer membrane protein	1006	110.8	185714	[a,b]	Outer membrane	
WP_046825240.1	TonB-dependent receptor	1139	126.1	156004		Outer membrane	
WP_046825949.1	TonB-dependent receptor	1036	115.3	115218		Outer membrane	
WP_080948648.1	TonB-dependent receptor	1038	117.4	64500	[a]	Outer membrane	
WP_052448976.1	TonB-dependent receptor	1067	117.5	44569	[a,b]	Outer membrane	
WP_046825332.1	TonB-dependent receptor	1002	111.5	30100	[a]	Outer membrane	
WP_052449101.1	TonB-dependent receptor	1062	119.5	24943		Outer membrane	
WP_052449125.1	TonB-dependent receptor	1041	115	22715	[a]	Outer membrane	
WP_052449008.1	TonB-dependent receptor	1144	128.3	19954		Outer membrane	
WP_052449020.1	TonB-dependent receptor	1103	121.7	19052		Outer membrane	
WP_046824757.1	SusC/RagA family TonB-linked outer membrane protein	1111	124.7	14148		Outer membrane	
WP_046825693.1	TonB-dependent receptor	1005	111.8	12991		Outer membrane	
WP_052449072.1	TonB-dependent receptor	1045	117.8	2405		Outer membrane	
ii. SusD/RagB homologous proteins (36/349)							
WP_046826242.1	RagB/SusD family nutrient uptake outer membrane protein	522	59.4	186027333	[a,b]	Outer membrane	O
WP_046825760.1	SusD/RagB family nutrient-binding outer membrane lipoprotein	517	58	123207333	[a,b]	Periplasmic	O
WP_046824472.1	RagB/SusD family nutrient uptake outer membrane protein	562	64.4	59171167	[a,b]	Periplasmic	O
WP_080948543.1	RagB/SusD family nutrient uptake outer membrane protein	495	56.7	54833617		Cytoplasmic	O
WP_014223517.1	SusD/RagB family nutrient-binding outer membrane lipoprotein	600	67.3	54486167	[a,b]	Extracellular	
WP_046825524.1	SusD/RagB family nutrient-binding outer membrane lipoprotein	626	71.1	48233833		Periplasmic	O
WP_046825921.1	RagB/SusD family nutrient uptake outer membrane protein	586	65.2	35447500	[a,b]	Periplasmic	O

(Continues)

TABLE 2 (Continued)

Accession	Definition	Amino acid	M.W. (kDa)	iBAQ	Previously reported proteins of Tf OMVs	Predicted subsellular location[c]	Lipoprotein[d]
WP_046824539.1	RagB/SusD family nutrient uptake outer membrane protein	396	45.2	31821167	[a,b]	Cytoplasmic	O
WP_046824486.1	RagB/SusD family nutrient uptake outer membrane protein	544	61.5	23265450	[a,b]	Periplasmic	O
WP_041590723.1	RagB/SusD family nutrient uptake outer membrane protein	508	58.2	21876000	[a]	Cytoplasmic	
WP_052299298.1	RagB/SusD family nutrient uptake outer membrane protein	486	55.4	21096333		Cytoplasmic	O
WP_046825094.1	RagB/SusD family nutrient uptake outer membrane protein	574	65.2	20940067	[a,b]	Outer membrane	O
WP_014225566.1	RagB/SusD family nutrient uptake outer membrane protein	527	58.5	18339733	[a,b]	Outer membrane	O
WP_014224710.1	SusD/RagB family nutrient-binding outer membrane lipoprotein	550	61.5	10070000	[a,b]	Periplasmic	O
WP_046825454.1	RagB/SusD family nutrient uptake outer membrane protein	483	54.1	7308650	[a,b]	Periplasmic	O
WP_052449116.1	RagB/SusD family nutrient uptake outer membrane protein	511	58.1	6149600		Periplasmic	O
WP_014224393.1	RagB/SusD family nutrient uptake outer membrane protein	629	71.2	5875962		Periplasmic	O
WP_014225706.1	RagB/SusD family nutrient uptake outer membrane protein	669	75.7	4128398	[a]	Outer membrane	O
WP_014225583.1	RagB/SusD family nutrient uptake outer membrane protein	568	65.1	3349985	[a]	Periplasmic	O
WP_046825367.1	RagB/SusD family nutrient uptake outer membrane protein	548	62.2	3324750	[a]	Periplasmic	O
WP_046824979.1	RagB/SusD family nutrient uptake outer membrane protein	631	73	3166467	[a]	Periplasmic	O
WP_014223948.1	RagB/SusD family nutrient uptake outer membrane protein	537	60.4	2572162	[a,b]	Outer membrane	O
WP_014226385.1	RagB/SusD family nutrient uptake outer membrane protein	546	63.4	1883928	[a,b]	Cytoplasmic	O
WP_041590902.1	RagB/SusD family nutrient uptake outer membrane protein	581	67.1	1768398	[b]	Outer membrane	O

(Continues)

TABLE 2 (Continued)

Accession	Definition	Amino acid	M.W. (kDa)	iBAQ	Previously reported proteins of Tf OMVs	Predicted subsellular location[c]	Lipoprotein[d]
WP_046825333.1	RagB/SusD family nutrient uptake outer membrane protein	519	58.4	1731037	[a]	Extracellular	O
WP_046825867.1	RagB/SusD family nutrient uptake outer membrane protein	503	57.6	1542047	[a]	Cytoplasmic	O
WP_161794928.1	SusD/RagB family nutrient-binding outer membrane lipoprotein	523	59.3	1528415		Outer membrane	
WP_161794959.1	SusD/RagB family nutrient-binding outer membrane lipoprotein	510	58.6	1128786		Periplasmic	O
WP_014226096.1	RagB/SusD family nutrient uptake outer membrane protein	627	71.3	876353	[a]	Periplasmic	
WP_046824781.1	RagB/SusD family nutrient uptake outer membrane protein	449	51	647263		Cytoplasmic	O
WP_201774589.1	RagB/SusD family nutrient uptake outer membrane protein	496	55	519212		Periplasmic	
WP_014224757.1	RagB/SusD family nutrient uptake outer membrane protein	521	58.7	483617	[a]	Outer membrane	
WP_046825741.1	RagB/SusD family nutrient uptake outer membrane protein	513	58.5	317818		Extracellular	O
WP_046825068.1	RagB/SusD family nutrient uptake outer membrane protein	590	67.7	316638		Cytoplasmic	
WP_046825184.1	RagB/SusD family nutrient uptake outer membrane protein	496	56.3	130706		Outer membrane	
WP_046825687.1	RagB/SusD family nutrient uptake outer membrane protein	672	76	7809	[a,b]	Outer membrane	O
iii. SusF/SusE homologous proteins (2/349)							
WP_080948653.1	SusF/SusE family outer membrane protein	461	49.8	7272283		Periplasmic	O
WP_161794973.1	SusF/SusE family outer membrane protein	379	41.8	6725433		Extracellular	O
iv. TonB and ExbB/ExbD (3/349)							
WP_014224380.1	MotA/TolQ/ExbB proton channel family protein	247	26.2	2854920	[a]	Inner Membrane	
WP_014224377.1	energy transducer TonB	232	25.5	1014317	[a]	Cytoplasmic	
WP_046826075.1	biopolymer transporter ExbD	197	22.4	125343		Periplasmic	

(Continues)

TABLE 2 (Continued)

Accession	Definition	Amino acid	M.W. (kDa)	iBAQ	Previously reported proteins of Tf OMVs	Predicted subsellular location[c]	Lipoprotein[d]
II. T9SS and its substrates (21/349)							
WP_087879716.1	PorT family protein	200	21.9	31880167		Periplasmic	
WP_161794962.1	PorT family protein	225	23.9	10765883		Outer membrane	
WP_052449061.1	Leucine-rich-repeat family virulence factor BspA	1081	113.7	9094583		Extracellular	
WP_041590792.1	type IX secretion system outer membrane channel protein PorV	392	43.5	3015000	a,b	Outer membrane	
WP_046825062.1	Leucine-rich repeat protein	1156	123.1	2980878	a,b	Periplasmic	
WP_161794970.1	T9SS type A sorting domain-containing protein	303	34.3	2665795		Periplasmic	
WP_046825257.1	hypothetical protein	1252	131	2418532	a,b	Extracellular	
WP_080948566.1	T9SS type A sorting domaincontaining protein	556	60.1	1851483		Extracellular	
WP_046825727.1	membrane protein	412	46.8	1237307	a,b	Outer membrane	
WP_046825848.1	T9SS type A sorting domain-containing protein	366	41.7	745872	a,b	Periplasmic	
WP_041590664.1	type IX secretion system protein PorQ	337	37.1	640450	a,b	Outer membrane	
WP_046824827.1	type IX secretion system sortase PorU	1143	127.5	541728	a,b	Outer membrane	O
WP_087879720.1	PorT family protein	220	25	411849		Outer membrane	
WP_046824969.1	PorT family protein	258	29	389717		Cytoplasmic	
WP_080948534.1	T9SS type A sorting domain-containing protein	948	105.1	279466		Outer membrane	
WP_080948639.1	PorT family protein	241	27	255083		Outer membrane	
WP_211346868.1	hypothetical protein	485	54.1	238797		Outer membrane	
WP_080948584.1	Ig-like domain-containing protein	1102	119.6	148972		Extracellular	
WP_046826144.1	T9SS type A sorting domain-containing protein	439	51.1	56241	a	Outer membrane	
WP_046825620.1	InlB B-repeat-containing protein, partial	764	44.4	51042	a	Outer membrane	
WP_052449111.1	hypothetical protein	769	84.6	41195	a,b	Extracellular	
III. Peptidases (32/349)							
WP_046824802.1	S41 family peptidase	1080	121.7	15396883	a,b	Periplasmic	
WP_046825904.1	S46 family peptidase	716	81.3	9029117	a,b	Cytoplasmic	
WP_041590581.1	Do family serine endopeptidase	502	54.1	8160883	a,b	Outer membrane	
WP_046824956.1	insulinase family protein	942	107.4	8140800	a,b	Cytoplasmic	

(Continues)

TABLE 2 (Continued)

Accession	Definition	Amino acid	M.W. (kDa)	iBAQ	Previously reported proteins of Tf OMVs	Predicted subsellular location[c]	Lipoprotein[d]
WP_046825514.1	M13 family metallopeptidase	677	77.2	3343550	[a,b]	Periplasmic	O
WP_201774585.1	S9 family peptidase	717	81.5	2372042		Outer membrane	O
WP_046826209.1	aminopeptidase	398	44.9	2118135	[a,b]	Extracellular	
WP_014225756.1	C69 family dipeptidase	546	61.7	1735003	[a,b]	Periplasmic	
WP_080948606.1	S41 Family peptidase	424	48.7	1342086	[a,b]	Outer membrane	
WP_046824727.1	M48 family metallopeptidase	264	28.9	1190647	[a]	Periplasmic	O
WP_052449065.1	M56 family metallopeptidase	480	53.9	1106950		Inner Membrane	
WP_046825797.1	dihydrofolate reductase	686	78.3	908190	[a,b]	Cytoplasmic	O
WP_046826048.1	prolyl oligopeptidase family serine peptidase	923	105.6	869057	[a]	Periplasmic	
WP_046825072.1	S41 family peptidase prolyl oligopeptidase family serine	477	54.1	598978		Outer membrane	O
WP_140230634.1	prolyl oligopeptidase family serine peptidase	689	78.1	517940		Periplasmic	
WP_046826150.1	S41 family peptidase	567	63.6	512090	[a]	Cytoplasmic	
WP_046824846.1	S41 family peptidase	432	49.3	456233	[a]	Outer membrane	
WP_014224179.1	S41 family peptidase	338	39	414159	[a,b]	Cytoplasmic	O
WP_046826215.1	carboxypeptidase-like regulatory domain-containing protein	764	88.2	305915	[a]	Outer membrane	
WP_014224429.1	C40 family peptidase	360	39.9	225154		Periplasmic	
WP_052449090.1	S9 family peptidase	846	95.7	209929		Outer membrane	
WP_087879727.1	M28 family peptidase	333	37.1	159647		Cytoplasmic	O
WP_046825437.1	S9 family peptidase	696	78.1	151529	[a]	Periplasmic	O
WP_046824550.1	carboxypeptidase-like regulatory domain-containing protein	875	97.7	139590		Outer membrane	
WP_046824629.1	S9 family peptidase	725	81.7	123663		Periplasmic	
WP_052449094.1	M56 family metallopeptidase	621	70.7	123307		Outer membrane	
WP_046824595.1	S41 family peptidase	532	60.2	74304		Cytoplasmic	
WP_052448955.1	transglutaminase	919	104	63324		Cytoplasmic	O
WP_046825299.1	outer membrane beta-barrel protein	773	86.9	58430		Outer membrane	
WP_046824921.1	S9 family peptidase	722	81.7	55747	[a]	Outer membrane	

(Continues)

TABLE 2 (Continued)

Accession	Definition	Amino acid	M.W. (kDa)	iBAQ	Previously reported proteins of Tf OMVs	Predicted subsellular location[c]	Lipoprotein[d]
WP_046825792.1	tail fiber domain-containing protein	362	39.5	39841	[a]	Outer membrane	
WP_046825809.1	peptidoglycan DD-metalloendopeptidase family protein	408	47	8483		Outer membrane	
IV. Glycosyl hydrolases (12/349)							
WP_046825029.1	family 20 glycosylhydrolase	777	86.5	5176950	[a,b]	Cytoplasmic	
WP_046826229.1	exo-alpha-sialidase	539	59.6	4718150	[a,b]	Outer membrane	
WP_014224118.1	glycoside hydrolase family 125 protein	489	55.9	1129365	[a,b]	Cytoplasmic	
WP_080948511.1	beta-glucosidase BglX	757	82.5	931922		Cytoplasmic	
WP_046826129.1	DUF4982 domain-containing protein	836	94.8	206253		Cytoplasmic	
WP_046826203.1	glycoside hydrolase family 97 protein	708	81.0	175357		Periplasmic	
WP_046825875.1	GH92 family glycosyl hydrolase	753	83.1	116603		Periplasmic	O
WP_046824466.1	family 10 glycosylhydrolase	514	60.2	97406		Cytoplasmic	
WP_087879742.1	glycoside hydrolase family 95 protein	837	93.7	81971		Cytoplasmic	
WP_014226077.1	glucosylceramidase	486	54.8	49757		Outer membrane	O
WP_087879739.1	family 10 glycosylhydrolase	471	53.0	34877		Periplasmic	
WP_046826115.1	GH92 family glycosyl hydrolase	766	87.7	30214	[a]	Extracellular	
V. Tetratricopeptide repeat proteins (10/349)							
WP_041590917.1	tetratricopeptide repeat protein	405	46.4	66361333	[a,b]	Periplasmic	
WP_046826085.1	tetratricopeptide repeat protein	563	61.9	53037333	[a,b]	Periplasmic	O
WP_046825261.1	tetratricopeptide repeat protein	999	114.4	3755017	[a,b]	Outer membrane	
WP_014226146.1	hypothetical protein	455	51.1	1664478	[a,b]	Periplasmic	
WP_046824990.1	tetratricopeptide repeat protein	573	63.5	1209542	[a]	Periplasmic	
WP_087879751.1	CDC27 family protein	490	56.0	652993		Cytoplasmic	
WP_080948616.1	tetratricopeptide repeat protein	594	68.2	160673		Cytoplasmic	
WP_046824917.1	tetratricopeptide repeat protein	353	39.7	49909		Cytoplasmic	O
WP_046825730.1	tetratricopeptide repeat protein	695	80.5	30143	[a]	Cytoplasmic	

(Continues)

TABLE 2 (Continued)

Accession	Definition	Amino acid	M.W. (kDa)	iBAQ	Previously reported proteins of Tf OMVs	Predicted subsellular location[c]	Lipoprotein[d]
WP_046824455.1	tetratricopeptide repeat protein	1160	134.7	7256		Cytoplasmic	O
VI. TolC family proteins (4/349)							
WP_052448970.1	TolC family protein	452	51.4	6720788		Outer membrane	
WP_052449039.1	TolC family protein	493	55.5	323811		Outer membrane	
WP_046825448.1	TolC family protein	463	52.0	195726	a,b	Cytoplasmic	
WP_046825612.1	TolC family protein	504	58.3	72056		Outer membrane	
VII. Chaperonin (3/349)							
WP_070098079.1	outer membrane protein assembly factor BamA	892	101.4	5748350		Outer membrane	
WP_041590894.1	outer membrane protein assembly factor BamD	268	31.7	2664600	a,b	Outer membrane	
WP_046825748.1	chaperonin GroEL	544	57.8	12160		Cytoplasmic	
VIII. Peroxidases (2/349)							
WP_014224706.1	glutathione peroxidase	199	22.5	10287100	a,b	Periplasmic	
WP_014225258.1	superoxide dismutase	194	22.0	1589670	a,b	Cytoplasmic	
IX. Proteins with domain of unknown function (22/349)							
WP_046825761.1	DUF5012 domain-containing protein	229	25.2	23340833	a,b	Outer membrane	O
WP_014225104.1	DUF4139 domain-containing protein	537	60.4	19909833	a	Cytoplasmic	
WP_046825355.1	DUF4831 family protein	356	39.7	10058367	a,b	Cytoplasmic	
WP_046824980.1	DUF1080 domain-containing protein	292	32.5	9225133	a,b	Periplasmic	O
WP_157755325.1	DUF4827 domain-containing protein	190	22.2	6351583		Cytoplasmic	
WP_014223783.1	DUF4270 domain-containing protein	472	54.4	5723692	a,b	Outer membrane	O
WP_080561855.1	DUF1080 domain-containing protein	421	48.3	4449033		Cytoplasmic	O
WP_161794927.1	DUF1573 domain-containing protein	482	52.8	2455607		Cytoplasmic	
WP_046826222.1	hypothetical protein	424	47.5	1967215	a,b	Periplasmic	O
WP_046825969.1	DUF3078 domain-containing protein	293	32.8	1751598	a	Outer membrane	
WP_046825940.1	DUF3858 domain-containing protein	544	61.4	1271043	a	Cytoplasmic	

(Continues)

TABLE 2 (Continued)

Accession	Definition	Amino acid	M.W. (kDa)	iBAQ	Previously reported proteins of Tf OMVs	Predicted subsellular location[c]	Lipoprotein[d]
WP_041590593.1	DUF4625 domain-containing protein	162	18.1	1233500	[a,b]	Periplasmic	O
WP_161794945.1	DUF5018 domain-containing protein	543	58.6	1229953		Outer membrane	O
WP_014224865.1	DUF4292 domain-containing protein	276	31.5	707153	[a]	Cytoplasmic	
WP_046825529.1	DUF1343 domain-containing protein	412	46.6	528335		Cytoplasmic	
WP_014225879.1	DUF3078 domain-containing protein	514	61.0	475055		Outer membrane	
WP_046825192.1	DUF1460 domain-containing protein	283	32.2	97464	[a,b]	Cytoplasmic	
WP_014225897.1	DUF5020 family protein	230	26.2	71250	[a]	Outer membrane	
WP_041591118.1	DUF1573 domain-containing protein	133	14.0	67737	[a]	Extracellular	
WP_046824883.1	DUF4876 domain-containing protein	411	45.9	60406		Periplasmic	O
WP_080948614.1	DUF4832 domain-containing protein	472	53.4	56351		Cytoplasmic	
X. Proteins without any reported domain (51/349)							
WP_087879763.1	DUF5103 domain-containing protein	417	48.9	30676		Outer membrane	
WP_140230695.1	hypothetical protein	227	25.0	95171833		Periplasmic	O
WP_046825523.1	hypothetical protein	284	32.5	76273333	[a,b]	Periplasmic	O
WP_152652238.1	ypothetical protein, partial	1533	22.2	31717500		Extracellular	
WP_041590592.1	hypothetical protein	126	13.3	24590500	[b]	Periplasmic	O
WP_046825842.1	hypothetical protein, partial	307	54.7	23300383	[b]	Cytoplasmic	
WP_140230593.1	ypothetical protein	1931	210.8	15707733		Extracellular	
WP_041590934.1	ypothetical protein	263	29.4	8019633	[a,b]	Periplasmic	O
WP_211346869.1	IgGFc-binding protein, partial	550	111.8	5419650		Extracellular	
WP_046826079.1	DUF4959 domain-containing protein	304	34.3	4912207		Periplasmic	
WP_046824517.1	hypothetical protein	1933	212.5	4634700	[a,b]	Extracellular	
WP_014225605.1	hypothetical protein	192	21.6	3883600	[a,b]	Cytoplasmic	

(Continues)

TABLE 2 (Continued)

Accession	Definition	Amino acid	M.W. (kDa)	iBAQ	Previously reported proteins of Tf OMVs	Predicted subsellular location[c]	Lipoprotein[d]
WP_140230685.1	hypothetical protein	259	29.2	3855750		Cytoplasmic	O
WP_046472582.1	DUF6242 domain-containing protein	452	50.5	3419483		Outer membrane	O
WP_140230599.1	hypothetical protein	373	42.5	3022180		Outer membrane	
WP_140230595.1	hypothetical protein	409	44.1	2817545		Cytoplasmic	
WP_075589073.1	hypothetical protein	287	33.6	2414268		Cytoplasmic	
WP_046825310.1	hypothetical protein	118	13.1	2231025	a,b	Cytoplasmic	O
WP_140230631.1	hypothetical protein	174	20.0	2197548		Periplasmic	
WP_046825699.1	hypothetical protein	141	15.8	1876625	a,b	Periplasmic	O
WP_046824888.1	hypothetical protein	404	44.5	1708545		Periplasmic	O
WP_140230681.1	hypothetical protein	1887	206.4	1694548		Extracellular	
WP_046826055.1	hypothetical protein	227	25.0	1196263	a,b	Inner membrane	
WP_046826124.1	hypothetical protein	494	54.7	1027338	a,b	Outer membrane	
WP_046824882.1	hypothetical protein	518	58.9	808682	a,b	Outer membrane	
WP_080948579.1	hypothetical protein	148	16.1	764434		Extracellular	
WP_046825277.1	hypothetical protein	601	68.3	713168		Outer membrane	
WP_046825307.1	hypothetical protein	202	22.9	698692	a,b	Extracellular	O
WP_140230660.1	hypothetical protein	366	42.1	687475		Outer membrane	
WP_046825081.1	hypothetical protein	288	33.0	672997		Cytoplasmic	O
WP_140230643.1	hypothetical protein	192	22.0	672995		Cytoplasmic	
WP_052448988.1	hypothetical protein	244	27.7	616285		Cytoplasmic	
WP_046825937.1	hypothetical protein	450	49.4	415118		Outer membrane	
WP_052449086.1	hypothetical protein	105	11.7	364795		Periplasmic	O
WP_014225797.1	hypothetical protein	125	14.3	277245		Cytoplasmic	O
WP_080948556.1	hypothetical protein	414	47.8	274272		Outer membrane	
WP_046824861.1	Hypothetical protein	156	17.6	228668	a,b	Cytoplasmic	O
WP_046826127.1	hypothetical protein	245	27.3	195270	a,b	Periplasmic	O
WP_140230692.1	hypothetical protein	365	41.5	176510		Cytoplasmic	
WP_014224149.1	hypothetical protein	794	92.8	169842		Outer membrane	
WP_014225414.1	Hypothetical protein	181	20.5	146538	a	Cytoplasmic	O
WP_046825935.1	hypothetical protein	210	23.4	87275	a,b	Outer membrane	
WP_046825562.1	hypothetical protein	336	39.2	84082		Cytoplasmic	
WP_052449091.1	hypothetical protein	290	33.1	70875	a	Cytoplasmic	
WP_140230609.1	hypothetical protein	215	25.5	58469		Outer membrane	
WP_014223749.1	hypothetical protein	197	22.5	54328		Cytoplasmic	

(Continues)

TABLE 2 (Continued)

Accession	Definition	Amino acid	M.W. (kDa)	iBAQ	Previously reported proteins of Tf OMVs	Predicted subsellular location[c]	Lipoprotein[d]
WP_046825757.1	DUF6345 domain-containing protein	536	60.4	43685		Outer membrane	
WP_014225170.1	hypothetical protein	228	25.8	38368		Cytoplasmic	
WP_004584866.1	MULTISPECIES: hypothetical protein	220	25.3	34967		Outer membrane	O
WP_046825649.1	spondin domain-containing protein	411	44.4	31659		Periplasmic	O
WP_087879764.1	hypothetical protein	308	35.5	24845		Outer membrane	
WP_046826164.1	hypothetical protein	540	61.2	20040		Outer membrane	O
XI. Others (96/349)							
WP_046825762.1	hypothetical protein	230	26.0	227381667	[a,b]	Periplasmic	O
WP_046825712.1	HmuY family protein	216	24.4	196977500	[a,b]	Periplasmic	O
WP_041590550.1	OmpA family protein	389	44.3	183211500	[a,b]	Periplasmic	
WP_014225890.1	TRL-like family protein	99	9.9	160931000	[a]	Extracellular	
WP_140230713.1	TlpA family protein disulfide reductase	363	42.0	70692333		Cytoplasmic	
WP_046824579.1	right-handed parallel beta-helix repeat-containing protein, partial	574	121.0	33376767	[b]	Extracellular	
WP_046825066.1	BT1926 family outer membrane beta-barrel protein	216	22.4	32672633	[a,b]	Outer membrane	
WP_046825745.1	OmpH family outer membrane protein	172	19.7	29373550	[a]	Periplasmic	
WP_041590627.1	SPOR domain-containing protein	156	17.6	28663500	[a,b]	Periplasmic	
WP_014224806.1	OmpH family outer membrane protein	164	18.9	26762333	[a,b]	Periplasmic	
WP_080948622.1	InlB B-repeat-containing protein	370	40.7	21761450		Periplasmic	O
WP_046825961.1	sugar phosphate isomerase/epimerase	297	33.7	17385633	[a,b]	Cytoplasmic	
WP_014226123.1	DUF4876 domain-containing protein	443	48.7	16323617	[a,b]	Extracellular	
WP_201774565.1	FKBP-type peptidyl-prolyl cis-trans isomerase	213	23.2	13956783		Periplasmic	
WP_046825546.1	carboxypeptidase-like regulatory domain-containing protein	418	48.5	13791583	[a]	Outer membrane	
WP_014224982.1	Ig-like domain-containing protein	540	58.4	13197050		Outer membrane	
WP_052449115.1	sugar phosphate isomerase/epimerase	328	36.7	12245267		Periplasmic	
WP_014223879.1	outer membrane protein transport protein	536	60.2	11065600	[a,b]	Outer membrane	

(Continues)

TABLE 2 (Continued)

Accession	Definition	Amino acid	M.W. (kDa)	iBAQ	Previously reported proteins of Tf OMVs	Predicted subsellular location[c]	Lipoprotein[d]
WP_046825843.1	PDZ domain-containing protein	473	54.7	9209083	[a,b]	Outer membrane	
WP_046826169.1	peptidylprolyl isomerase	453	52.4	8070333		Cytoplasmic	
WP_014223614.1	copper resistance protein NlpE	144	15.7	7889900	[a,b]	Cytoplasmic	O
WP_046824745.1	FKBP-type peptidyl-prolyl cis-trans isomerase	196	21.4	7822617	[a,b]	Periplasmic	O
WP_014224852.1	peptidylprolyl isomerase	532	61.5	7764483	[a,b]	Cytoplasmic	
WP_014225065.1	thioredoxin	151	16.9	6322092	[a]	Periplasmic	
WP_014225134.1	Gfo/Idh/MocA family oxidoreductase	493	54.6	5504667	[a,b]	Periplasmic	
WP_046825424.1	DUF1080 domain-containing protein	1158	126.5	4902217	[a,b]	Periplasmic	
WP_046824717.1	endonuclease/exonuclease/phosphatase family protein	278	31.4	4778542	[a,b]	Cytoplasmic	
WP_014225136.1	NigD-like protein	249	28.4	4543683		Periplasmic	
WP_046824488.1	alkaline phosphatase	562	62.5	4349833	[a,b]	Periplasmic	
WP_046824809.1	hypothetical protein	366	40.3	4050568	[a,b]	Extracellular	O
WP_046824516.1	AhpC/TSA family protein	371	40.9	3964183		Cytoplasmic	O
WP_046824554.1	OmpA family protein	228	23.8	3590417	[a,b]	Periplasmic	O
WP_046825948.1	SGNH/GDSL hydrolase family protein	256	28.6	3299150	[a,b]	Periplasmic	
WP_046825312.1	discoidin domain-containing protein	1209	136.7	3146430	[a]	Extracellular	O
WP_014225524.1	metallophosphoesterase family protein	335	37.5	3112372	[a,b]	Cytoplasmic	
WP_046825011.1	peptidylprolyl isomerase	224	25.2	2741710		Cytoplasmic	
WP_046824476.1	TIM barrel protein	296	32.9	2718233	[a,b]	Cytoplasmic	
WP_014223776.1	hypothetical protein	116	13.4	2367673		Cytoplasmic	O
WP_014224736.1	glucosaminidase domain-containing protein	323	37.5	2316012	[a]	Outer membrane	
WP_140230687.1	hypothetical protein	370	40.1	2134147		Periplasmic	
WP_046825560.1	Gfo/Idh/MocA family oxidoreductase	468	51.8	1821627	[a]	Periplasmic	
WP_046825320.1	Omp28-related outer membrane protein	519	57.4	1774808	[a]	Extracellular	O
WP_046825205.1	polysaccharide biosynthesis/export family protein	269	30.2	1643552		Inner Membrane	O
WP_046826099.1	alpha/beta hydrolase	294	32.5	1601658		Cytoplasmic	
WP_014225403.1	GLPGLI family protein	284	32.3	1590168		Periplasmic	
WP_046825728.1	alkaline phosphatase family protein	528	59.9	1567102	[a]	Cytoplasmic	
WP_014225175.1	hypothetical protein	289	32.8	1414502	[a]	Outer membrane	O

(Continues)

TABLE 2 (Continued)

Accession	Definition	Amino acid	M.W. (kDa)	iBAQ	Previously reported proteins of Tf OMVs	Predicted subsellular location[c]	Lipoprotein[d]
WP_046825563.1	VIT domain-containing protein	974	111.3	1365832	[a]	Cytoplasmic	
WP_014225844.1	alginate export family protein	429	49.5	1325832	[a]	Outer membrane	
WP_046825513.1	SGNH/GDSL hydrolase family protein	571	64.7	1305759	[a]	Cytoplasmic	
WP_014225762.1	FKBP-type peptidyl-prolyl cis-trans isomerase	238	25.3	1298790	[a]	Periplasmic	O
WP_046826220.1	flavodoxin	188	21.0	1296548	[a,b]	Periplasmic	
WP_046825170.1	MG2 domain-containing protein	1864	207.5	1096802		Outer membrane	O
WP_014223958.1	AhpC/TSA family protein	203	22.4	1090317	[a,b]	Periplasmic	
WP_014224160.1	Gfo/Idh/MocA family oxidoreductase	418	47.1	996650	[a,b]	Periplasmic	
WP_046826137.1	hypothetical protein	717	78.8	987103	[a,b]	Outer membrane	O
WP_046824479.1	outer membrane beta-barrel protein	155	17.1	969000	[a]	Outer membrane	
WP_052448969.1	DUF4981 domain-containing protein	1129	128.3	869488		Extracellular	
WP_046826224.1	sirohydrochlorin cobaltochelatase	311	35.2	820347	[a,b]	Cytoplasmic	
WP_052449099.1	DUF3857 domain-containing protein	648	72.8	727815		Periplasmic	
WP_004585095.1	MULTISPECIES: GLPGLI family protein	238	27.0	691407		Cytoplasmic	
WP_178387126.1	InlB B-repeat-containing protein, partial	386	23.2	675220		Periplasmic	
WP_014225615.1	patatin-like phospholipase family protein	767	87.7	657152		Outer membrane	
WP_046825606.1	porin	381	42.6	642137	[a]	Outer membrane	
WP_087879733.1	Ig-like domain-containing protei	356	36.8	592833		Extracellular	
WP_046826227.1	GDSL-type esterase/lipase family protein	692	78.5	562303		Cytoplasmic	
WP_046825543.1	hypothetical protein	507	57.6	510352		Outer embrane	
WP_087879745.1	xanthan lyase	1001	112.1	425337		Outer membrane	
WP_046824688.1	TraB/GumN family protein	319	36.6	349438	[a]	Cytoplasmic	O
WP_014224694.1	gliding motility protein GldN	370	42.6	315555	[a]	Periplasmic	
WP_046825182.1	glycosyl hydrolase family 28 protein	493	54.9	310960	[a]	Cytoplasmic	
WP_041590639.1	galactose mutarotase	376	41.2	295625	[a,b]	Extracellular	O
WP_161794960.1	LamG domain-containing protein	263	28.7	244461		Periplasmic	O

(Continues)

TABLE 2 (Continued)

Accession	Definition	Amino acid	M.W. (kDa)	iBAQ	Previously reported proteins of Tf OMVs	Predicted subsellular location[c]	Lipoprotein[d]
WP_080948644.1	Ig-like domain-containing protein	634	65.9	214638		Outer membrane	
WP_052448942.1	gliding motility-associated C-terminal domain-containing protein	440	49.6	184677		Extracellular	
WP_041591331.1	glycerophosphodiester phosphodiesterase	260	29.6	161748	[a]	Cytoplasmic	
WP_080948640.1	hypothetical protein	446	51.2	157509		Cytoplasmic	
WP_201774570.1	FAD-dependent oxidoreductase	528	59.0	149364		Cytoplasmic	
WP_014226380.1	YtxH domain-containing protein	111	12.2	135322		Periplasmic	
WP_046825839.1	hypothetical protein	467	53.9	127972	[a,b]	Cytoplasmic	O
WP_046824878.1	alpha-L-rhamnosidase	911	102.9	86377		Extracellular	O
WP_046824591.1	bifunctional metallophosphatase/5′-nucleotidase	478	53.8	62178		Cytoplasmic	
WP_046824784.1	SUMF1/EgtB/PvdO family nonheme iron enzyme	479	54.9	53363		Extracellulam	O
WP_014223652.1	preprotein translocase subunit YajC	112	12.1	51502		Inner membrane	
WP_046824463.1	LysM peptidoglycan-binding domain-containing protein	596	68.4	47889		Outer membrane	
WP_046825315.1	membrane protein	214	23.9	41528	[a]	Outer membrane	
WP_080948611.1	alpha/beta fold hydrolase	455	49.8	39991		Cytoplasmic	
WP_080948582.1	fibronectin type III domain-containing protein	606	66.5	37536		Periplasmic	
WP_046824940.1	erythromycin esterase family protein	610	70.5	28957		Cytoplasmic	
WP_046825018.1	cell surface protein SprA	2482	282.0	25632		Outer membrane	
WP_014225032.1	alpha/beta hydrolase-fold protein	565	66.6	25597	[a]	Periplasmic	
WP_046825480.1	nitroreductase	228	25.1	24553		Periplasmic	O
WP_052449031.1	lamin tail domain-containing protein	473	52.2	15418		Extracellular	
WP_014225269.1	elongation factor Tu	395	43.3	10343		Cytoplasmic	
WP_046824756.1	zinc-dependent metalloprotease	876	99.3	7514		Cytoplasmic	
WP_052449025.1	TANFOR domain-containing protein	3078	343.6	4576		Periplasmic	

[a]The *T. forsythia* OMVs protein previously reported by Veith et al. (2015).
[b]The *T. f orsythia* OMVs protein previously reported by Friedrich et al. (2015).
[c]The subcellular location of each protein was predicted by CELLO v.2.5 (Molecular Bioinformatics Center of National Chiao Tung University).
[d]The lipid attachment site of each protein was predicted by ExPASy—PROSITE database.

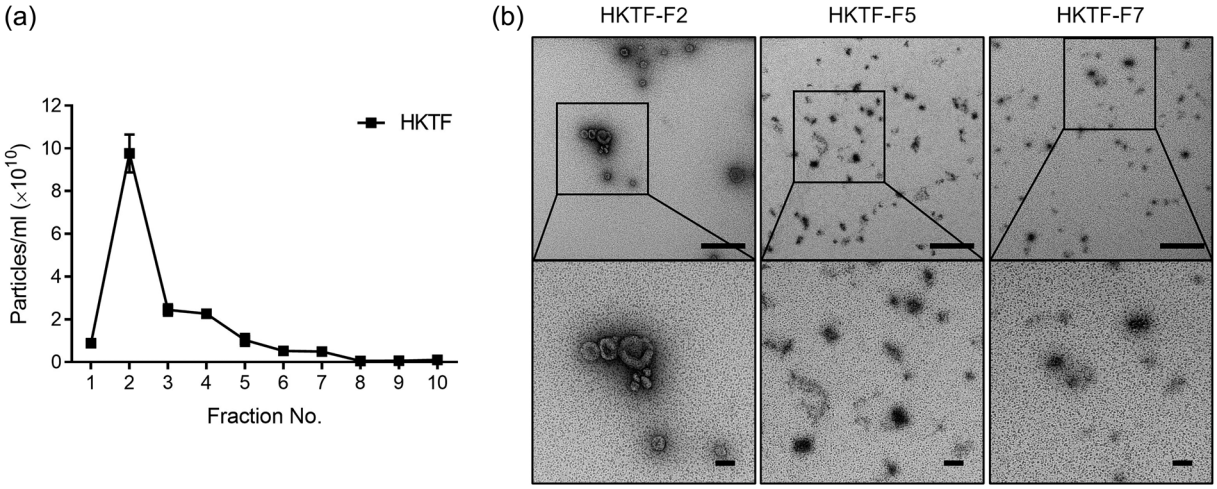

FIGURE 4 Characterisation of the EVs derived from the CM of macrophages treated with heat-killed *T. forsythia*. (a) Nanoparticle concentrations in each density gradient fraction were analysed by NTA. (b) The indicated fractions were negatively stained and imaged by TEM. Scale bar: 500 nm for wide-field images and 100 nm for close-up images. The experiments were performed at least three times independently. HKTF, Heat-killed *T. forsythia* treatment group.

family proteins. Three proteins (0.9%) were chaperonins, and two proteins (0.6%) were peroxidases. Twenty-two proteins (6.3%) had domains of unknown function. Fifty-one proteins (14.6%) did not have any reported domains. Detailed information on the TF-F5 *T. forsythia* proteins is listed in Table 2.

3.3 | The conditioned medium of the macrophages enhanced EV release from *T. forsythia*

To verify that the EVs in TF-F5 were released from live *T. forsythia*, we isolated and characterised the EVs derived from the CM of macrophages treated with heat-killed *T. forsythia* (Figure 4). NTA showed that the nanoparticles were not enriched in F5 (Figure 4a). TEM images also showed that vesicular structures were detected in F2 but not in F5 (Figure 4b). These results indicate that *T. forsythia* EVs were released from live bacteria under the macrophage infection.

Bacteria regulate the release of EVs to adapt to changes in their surroundings (Schwechheimer & Kuehn, 2015). Encounters with macrophages can be stressful for *T. forsythia* because macrophages are sentinels against microbial infection and nutrients available in CM may not be sufficient for the growth of *T. forsythia*. To identify whether the CM of THP-1 macrophages influence the release of EVs from *T. forsythia*, we incubated live *T. forsythia* in the EV-free CM of the macrophages and then isolated the EVs (Figure 5a). The EVs in the CM of the non-infected and *T. forsythia*-infected macrophages were eliminated by 100 kDa MWCO ultrafiltration. The EV-free CM from the non-infected macrophages and the *T. forsythia*-infected macrophages were designated NI-100K and TF-100K, respectively. NTA confirmed that NI-100K and TF-100K were free of nanoparticles (data not shown). Interestingly, *T. forsythia* released EVs in the NI-100K and TF-100K medium but not in the fresh RPMI 1640 medium (Figure 5b). *T. forsythia* cultured in TF-100K released more EVs than *T. forsythia* cultured in NI-100K (Figure 5b). TEM images and immunoblotting showed that F5 was enriched with vesicles and *T. forsythia* proteins (Figure 5c,d). These results suggest the following: first, the CM of the THP-1 macrophages was stressful to *T. forsythia*; second, the EVs in TF-F5 were directly released from *T. forsythia*, not from infected macrophages; and third, unknown soluble molecules under 100 kDa in the CM of the macrophages promoted *T. forsythia* to release EVs.

3.4 | EVs derived from *T. forsythia*-infected macrophages induced a pro-inflammatory response

Bacterial EVs as well as host EVs can transfer their biological molecules to host recipient cells (Palomino et al., 2021; Shao et al., 2020). Therefore, we investigated the inflammatory responses of the EVs in TF-F2 and TF-F5 by measuring the expression of pro-inflammatory cytokines in THP-1 macrophages including TNF-α, IL-1β, IL-6 and IL-8. For negative controls, RPMI complete medium without EVs treatment were used (non-treatment, NT). When THP-1 macrophages were treated with TF-F2, the expression level of TNF-α was significantly higher than that of the cells treated with NI-F2 (Figure 6). There was no significant difference in the expression levels of IL-1β, IL-6 and IL-8 between the NI-F2- and TF-F2-treated macrophages. Although TF-F2 itself had significant amounts of TNF-α, IL-β and IL-8 (Table 1 and Figure 3c), these cytokines were not detected by ELISA at the concentration of 1×10^9 particles/mL (data not shown).

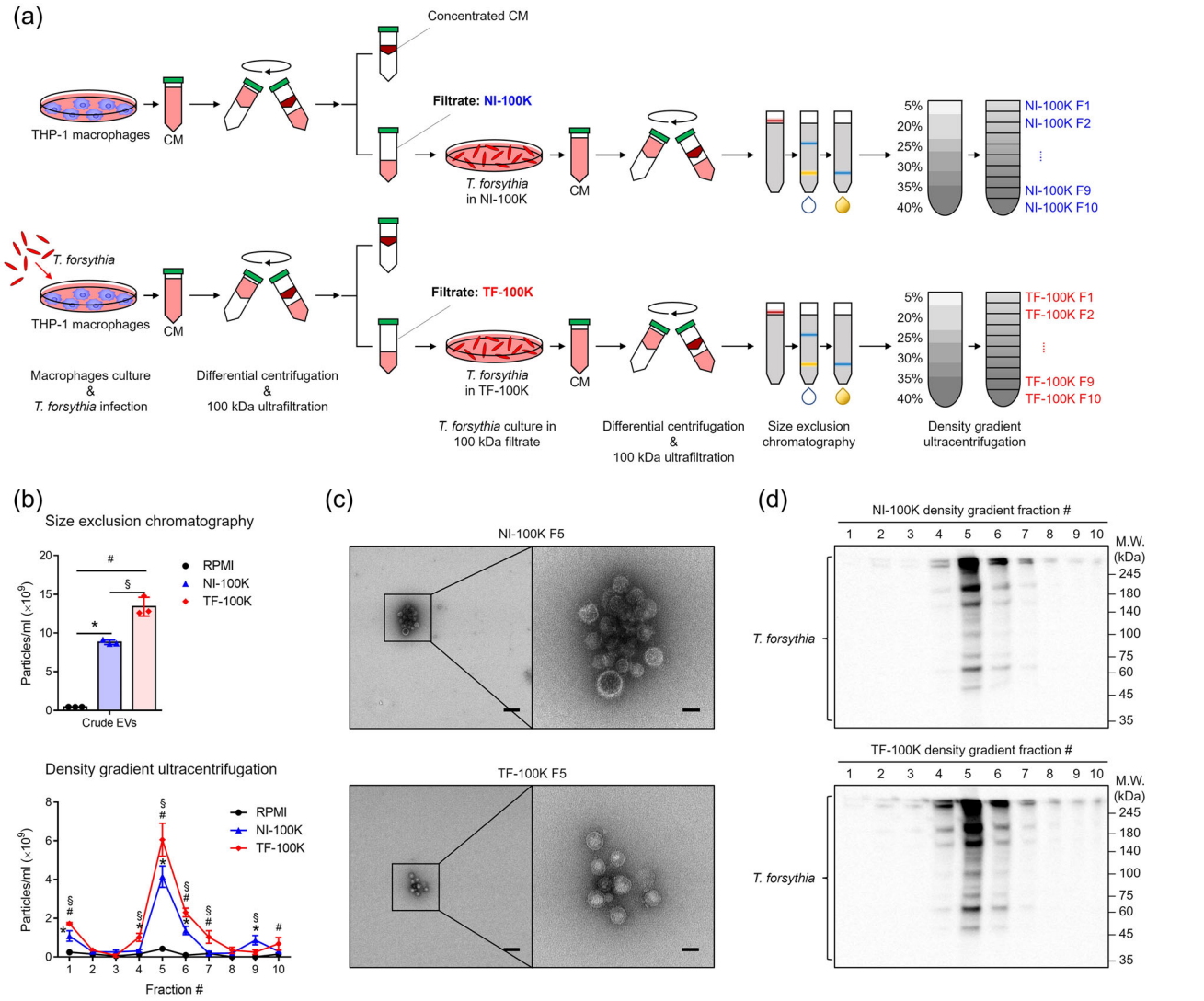

FIGURE 5 Identification of the OMVs released from live *T. forsythia* cultured in the CM of macrophages. (a) Schematic diagram of the *T. forsythia* incubation in the EV-free macrophage CM. (b) Nanoparticle concentrations of the crude EVs (upper panel) and density gradient fractions (lower panel) were analysed by NTA. (c) The indicated fractions were negatively stained and imaged by TEM. Scale bar: 200 nm for wide-field images and 50 nm for close-up images. (d) Immunoblotting results of the density gradient fractions using a *T. forsythia*-specific antibody. The experiments were performed at least three times independently. The data are presented as the mean ± standard deviation of triplicate assays and were analysed by one-way and two-way ANOVA. $^{*}p < 0.05$ compared between NI-100K and RPMI, $\#p < 0.05$ compared between TF-100K and RPMI and $\S p < 0.05$ compared between NI-100K and TF-100K.

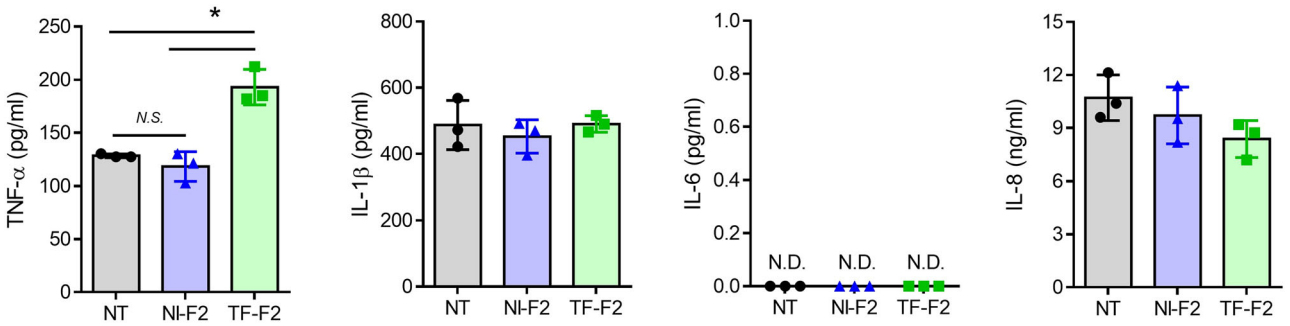

FIGURE 6 Pro-inflammatory cytokines induced by the macrophage-derived EVs. THP-1 macrophages were treated with NI-F2 and TF-F2 EVs (1×10^9 particles/mL) for 4 h, respectively. For negative controls (NT, non-treatment), cell culture medium (RPMI complete medium) was used. After treatment period, the expression level of TNF-α, IL-1β, IL-6 and IL-8 in the culture supernatants were measured by ELISA. The experiments were performed at least three times independently. The data are presented as the mean ± standard deviation of triplicate assays and were analysed by one-way ANOVA. NT, non-treatment group; N.D., not detected; N.S., not significant. $^{*}p < 0.05$.

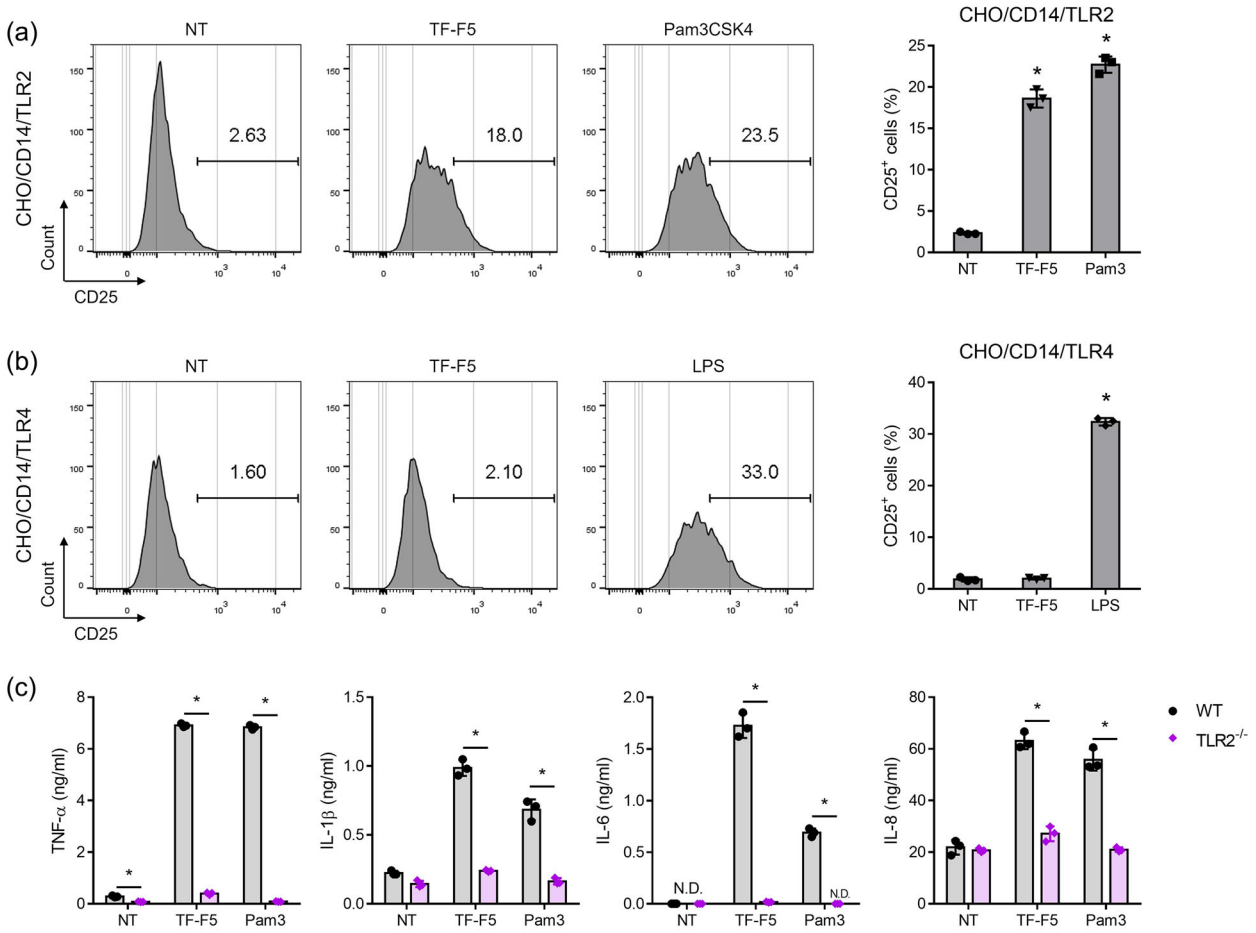

FIGURE 7 TLR2-mediated activation of pro-inflammatory responses induced by the *T. forsythia*-derived EVs. (a) CHO/CD14/TLR2 and (b) CHO/CD14/TLR4 cells were stimulated with TF-F5 (1×10^9 particles/mL) and Pam3CSK4 (100 ng/mL) or ultrapure LPS (100 ng/mL) for 20 h. The expression level of CD25 on the cells by TLR activation was measured by flow cytometry. For NT, complete cell culture medium (Ham's F-12 Nutrient complete medium) was used. (c) THP-1 WT and TLR2$^{-/-}$ macrophages were treated with TF-F5 (1×10^9 particles/mL) and Pam3CSK4 (10 ng/mL) for 24 h. For NT, cell culture medium (RPMI complete medium) was used. The expression levels of TNF-α, IL-1β, IL-6 and IL-8 in the culture supernatant were measured by ELISA. The experiments were performed at least three times independently. The data are presented as the mean ± standard deviation of triplicate assays and were analyzed by one-way and two-way ANOVA. NT, non-treatment group; N.D., not detected; Pam3, Pam3CSK4-treatment group; LPS, Ultrapure LPS-treatment group. $^*p < 0.05$.

To investigate the immunostimulatory effect of *T. forsythia* virulence factors in TF-F5, we treated TF-F5 with CHO/CD14/TLR2 and CHO/CD14/TLR4 reporter cells. TF-F5 activated TLR2 but did not activate TLR4 (Figure 7a,b). To confirm whether TF-F5 stimulates host cells through TLR2, the wild type (WT) and TLR2$^{-/-}$ THP-1 macrophages were treated with TF-F5, and the expression levels of pro-inflammatory cytokines were measured by ELISA. TF-F5 significantly induced TNF-α, IL-1β, IL-6 and IL-8 in the WT THP-1 macrophages but not in the TLR2$^{-/-}$ macrophages (Figure 7c). These results indicate that TF-F5 stimulates host cells to release pro-inflammatory cytokines through the TLR2 signalling pathway.

4 | DISCUSSION

In this study, we characterised EVs derived from the CM of *T. forsythia*-infected macrophages by proteome and immunostimulatory response analyses. The macrophage-derived EVs carried pro-inflammatory cytokines and inflammatory mediators that are associated with the pathogenesis of periodontitis and the activation of immune cells. The *T. forsythia*-derived OMVs had bacterial virulence factors that activated the TLR2 signalling pathway and increased the pro-inflammatory response in host cells. The release of EVs is one of the mechanisms that release virulence factors of periodontal pathogens, which can induce host pro-inflammatory responses. Similar to our study, two distinct EVs with different densities were released from macrophages infected with *Mycobacterium tuberculosis*, the causative agent of tuberculosis (Athman et al., 2015). The EVs derived from *M. tuberculosis* contained lipoproteins and lipoglycans and induced IL-8 from HEK293/hTLR2-CD14 and TNF-α from murine macrophages.

However, in that study, macrophage-derived EVs did not induce cytokines, and proteome analysis for these two distinct EVs was not conducted. Elsayed et al. reported that EVs released from dendritic cells (DCs) infected with *Porphyromonas gingivalis*, a keystone periodontal pathogen, were isolated by ultracentrifugation without density gradient purification and showed that EVs contained age-related miRNAs, IL-1β, TNF-α, IL-6 and fimbrial adhesin protein mfa1, inducing premature senescence in DCs (Elsayed et al., 2021). Our study is distinct from these studies in that proteome analysis of the bacterial and host cell-derived EVs was conducted, and host cell-derived EVs significantly induced TNF-α.

The inflammatory nature of TF-F2 was confirmed through an in vitro experiment and proteome analysis. TF-F2 significantly induced TNF-α secretion from the macrophages. According to the GOBP term, TF-F2 is enriched with proteins associated with neutrophil/granulocyte activation, leukocyte-mediated immunity and secretion. Additionally, TF-F2 contained various proteins that play a role in the pathogenesis of periodontitis. Among the proteins increased in TF-F2, the expression levels of TNF-α, IL-8 and IL-1β were remarkably high. These pro-inflammatory cytokines are frequently detected in the saliva or gingival crevicular fluid of patients with chronic periodontitis (Gomes et al., 2016; Noh et al., 2013). TNF-α and IL-1β are associated with several inflammatory events, including the induction of adhesion molecules and other mediators that facilitate and amplify the inflammatory response, the stimulation of matrix metalloproteinase, and bone resorption (Graves & Cochran, 2003). IL-8 is a chemoattractant cytokine that recruits neutrophils, which are the major population of immigrant cells in periodontitis and are responsible for the destruction of periodontal tissues (Bickel, 1993). SPP1 enhances the production of IL-12 from DCs and IFN-γ from T cells (Renkl et al., 2005). Similar to a previous report, *T. forsythia* OMV-stimulated DCs produced IL-12 and polarised naïve $CD4^+$ T cells to IFN-γ^+IL-$17A^-CD4^+$ T cells (Lim et al., 2022). Although the role of SPP1 was not evaluated in the study, it seems that SPP1 plays a role in IL-12 production by DCs and Th1 polarisation. MMP9 plays a major role in connective tissue destruction and is one of the major biomarkers of periodontitis (Luchian et al., 2022). Therefore, when macrophages are infected with *T. forsythia*, they release inflammatory EVs that contribute to the progression of periodontitis.

We believe that TNF-α, IL-8 and IL-1β in TF-F2 are vesicular proteins rather than soluble secreted protein contamination for the following reasons: first, majority of non-vesicular soluble cytokines/chemokines could be eliminated during the EV isolation procedure, including 100 kDa ultrafiltration, size exclusion chromatography and buoyant density gradient ultracentrifugation, (Dhondt et al., 2020; Shu et al., 2019), since the size of cytokines/chemokines is relatively small (TNF-α, 17.3 kDa; IL-8, 8.9 kDa; pro-IL-1β, 31 kDa; mature-IL-1β, 17 kDa); second, TF-F2 contained specific cytokines/chemokines such as TNF-α, IL-8 and IL-1β, but did not contain other cytokines/chemokines, including IL-6, IL-10 and CXCL10, which are highly secreted from THP-1 macrophages upon *T. forsythia* infection (Chinthamani et al., 2022); and third, although cytokines are soluble factors secreted by cells, cytokines can be encapsulated in EVs derived from diverse cell types and body fluids (Fitzgerald et al., 2018). There were differences between the subcellular localisation prediction based on protein sequences and the cellular component enrichment analysis. This distinction suggested that many proteins could be packaged in EVs and transported out of the cell from their original location. TNF-α, IL-8 and IL-1β had not yet been annotated in extracellular exosomes (GO:0070062), but we anticipated that these proteins would soon be annotated through additional research.

In the present study, we identified unknown soluble factors under 100 kDa in the CM of the macrophages promoted *T. forsythia* to release OMVs. Some molecules might be involved in this phenomenon. First, antimicrobial peptides (AMPs) might affect OMV release from *T. forsythia*. AMP treatment induces OMVs production in *Escherichia coli* (Manning & Kuehn, 2011; Balhuizen et al., 2021). Second, reactive oxygen species (ROS) are known as inducer for releasing OMVs in *Neisseria meningitidis*, *Pseudomonas aeruginosa* and *Helicobacter pylori* (Lekmeechai et al., 2018; Macdonald & Kuehn, 2013; van de Waterbeemd et al., 2013). OMV production from bacterial cells seems to be one of the bacterial defence mechanisms against host innate immune responses. OMVs showed neutralising activity against AMP-mediated bacteria killing (Balhuizen et al., 2021; Manning & Kuehn, 2011). Also, release of OMVs can reduce ROS-mediated oxidative stress in bacteria (Schwechheimer & Kuehn, 2015). We speculated that *T. forsythia* OMVs might act as bacterial defence mechanisms against host innate immune responses.

Bacterial EVs are enriched with various virulence factors that can trigger inflammatory responses in hosts. In the present study, we demonstrated that *T. forsythia*-derived OMVs (TF-F5) induced pro-inflammatory responses and activated the TLR2 signalling pathway. Diverse microbe-associated molecular patterns of *T. forsythia*-derived OMVs might be responsible for pro-inflammatory responses through the TLR2 signalling pathway. In-depth quantitative proteomic analysis identified several TLR2 agonists in the *T. forsythia*-derived OMVs including 95 bacterial lipoproteins and leucine-rich-repeat family virulence factor BspA (WP_052449061.1). Bacterial lipoproteins are produced by all bacteria and are known as major TLR2 ligands (Oliveira-Nascimento et al., 2012). BspA of *T. forsythia* activates TLR2 and induces pro-inflammatory cytokines from macrophages (Myneni et al., 2012). In addition, exo-alpha-sialidase (WP_046826229.1), beta-glucosidase BglX (WP_080948511.1), family 20 glycosyl hydrolase (HexA; WP_046825029.1), chaperonin GroEL (WP_046825748.1) and two S9 family peptidases (WP_046825437.1 and WP_046824629.1), which are non-TLR2 agonist virulence factors related to the pathogenesis of periodontal diseases, were also identified in the *T. forsythia*-derived OMVs. Glycosyl hydrolases, including exo-alpha-sialidase, BglX, and family 20 glycosyl hydrolase, might play a role in the disruption of periodontal tissue and support the growth of other oral bacteria nearby since they hydrolyse oligosaccharides and proteoglycans in periodontal tissue, gingival crevicular fluid, or saliva (Sharma, 2010). Chaperonin GroEL (WP_046825748.1) induces a pro-inflammatory response and synergizes with IL-17 for inflammatory bone resorption (Jung et al., 2017). S9 family peptidases, also known as dipeptidyl peptidase IV (DppIV), are serine proteases that degrade the collagen of the periodontium during periodontitis progression (Yost & Duran-Pinedo, 2018). Therefore, we believe

that when periodontal pathogens encounter innate immune cells, periodontal pathogens release EVs with virulence factors that can induce both local and systemic inflammatory responses without cell-to-cell interactions.

The release of EVs is one of the survival strategies of bacteria in terms of nutrient utilisation (Caruana & Walper, 2020; Liu et al., 2018). There were several proteins that may play a role in nutrient uptake and utilisation in *T. forsythia*-derived OMVs. RagB/SusD homologous proteins combine with their counterpart TonB-dependent receptors and capture specific nutrients in the environment and then transport them into cells (Bolam & van den Berg, 2018). HmuY family protein (WP_046825712.1), also known as Tfo, is a heme-binding protein and is upregulated under low-iron/heme conditions in both *T. forsythia* whole cells and OMVs (Bielecki et al., 2018). Heme is required for the optimal growth of *T. forsythia* and other periodontal pathogens (Yoo & Lee, 2021). *T. forsythia* might release OMVs to capture nutrients in the microenvironment, and that through the uptake of these EVs, *T. forsythia* or nearby periodontal pathogens utilise the nutrients captured in the EVs for their own survival. However, vesicles from other bacteria including non-oral bacteria need to be analysed to conclude that *T. forsythia* OMVs specifically contribute to nutrient uptake.

A major limitation of this study is that we used only THP-1 cells, a human innate immune cell line, to characterise the biological feature of EVs upon infection with the human periodontal pathogen *T. forsythia*. The pathogenic role of EVs from *T. forsythia*-infected macrophages and *T. forsythia*-derived OMVs needs to be investigated in animal periodontitis models. Recently, there have been several trials aiming to induce periodontitis and assess inflammatory responses in the periodontal tissues using silk thread ligation with OMVs derived from periodontal pathogens, including *Fusobacterium nucleatum* and *P. gingivalis* (Chen et al., 2022; Fan et al., 2023). Although we did not evaluate the inflammatory responses of EVs on the periodontal tissues, we believe that the EVs released from immune cells and periodontal pathogens of inflamed periodontal tissues may freely disseminate to systemic sites and induce inflammation. Indeed, systemic injection of *T. forsythia* OMV remarkably increased TNF-α (data not shown). Therefore, it is worthwhile to assess the EVs from periodontal pathogen-infected immune cells and EVs from each periodontal pathogen in the pathogenesis of periodontitis.

In summary, we demonstrated that two distinct EVs were derived from *T. forsythia*-infected human macrophages and that the CM of the macrophages promoted *T. forsythia* to release EVs. The macrophage-derived EVs carried pro-inflammatory cytokines and immune mediators that played a role in the inflammatory responses during periodontitis progression. The *T. forsythia*-derived OMVs contained virulence factors and induced pro-inflammatory responses by TLR2 activation. Therefore, not only macrophage-derived EVs but also *T. forsythia*-derived OMVs might be responsible for immune responses in local periodontal tissues and other systemic organs by spreading through the bloodstream. Taken together, EVs might be a useful tool for understanding the pathogenic mechanisms of periodontal pathogens.

AUTHOR CONTRIBUTIONS

Younggap Lim: Conceptualization; data curation; formal analysis; project administration; investigation; methodology; writing—original draft. **Hyun Young Kim**: Funding acquisition; writing—review and editing. **Dohyun Han**: Data curation; formal analysis; funding acquisition; investigation; writing—review and editing. **Bong-Kyu Choi**: Conceptualization; funding acquisition; project administration; supervision; writing—review and editing.

ACKNOWLEDGEMENTS

This work was supported by grants from the National Research Foundation of Korea (NRF-2020R1A5A1019023, NRF-2021R1A2C1003952 and NRF-2022R1C1C2007752), the Dental Research Institute of Seoul National University, and the SNUH Research Fund (2620210020).

CONFLICT OF INTEREST STATEMENT

The authors declare that they have no competing interests.

ORCID

Bong-Kyu Choi https://orcid.org/0000-0003-3743-7209

REFERENCES

Arteaga-Blanco, L. A., & Bou-Habib, D. C. (2021). The role of extracellular vesicles from human macrophages on host-pathogen interaction. *International Journal of Molecular Sciences*, *22*(19), 10262.

Athman, J. J., Wang, Y., McDonald, D. J., Boom, W. H., Harding, C. V., & Wearsch, P. A. (2015). Bacterial membrane vesicles mediate the release of *Mycobacterium tuberculosis* lipoglycans and lipoproteins from infected macrophages. *Journal of Immunology (Baltimore, Md. : 1950)*, *195*(3), 1044–1053. https://doi.org/10.4049/jimmunol.1402894

Balhuizen, M. D., van Dijk, A., Jansen, J. W. A., van de Lest, C. H. A., Veldhuizen, E. J. A., & Haagsman, H. P. (2021). Outer membrane vesicles protect gram-negative bacteria against host defense peptides. *mSphere*, *6*(4), e0052321. https://doi.org/10.1128/mSphere.00523-21

Bickel, M. (1993). The role of interleukin-8 in inflammation and mechanisms of regulation. *Journal of Periodontology*, *64*, (5 Suppl), 456–460.

Bielecki, M., Antonyuk, S., Strange, R. W., Smalley, J. W., Mackiewicz, P., Śmiga, M., Stępień, P., Olczak, M., & Olczak, T. (2018). *Tannerella forsythia* Tfo belongs to *Porphyromonas gingivalis* HmuY-like family of proteins but differs in heme-binding properties. *Bioscience Reports*, *38*(5), BSR20181325. https://doi.org/10.1042/BSR20181325

Bittel, M., Reichert, P., Sarfati, I., Dressel, A., Leikam, S., Uderhardt, S., Stolzer, I., Phu, T. A., Ng, M., Vu, N. K., Tenzer, S., Distler, U., Wirtz, S., Rothhammer, V., Neurath, M. F., Raffai, R. L., Günther, C., & Momma, S. (2021). Visualizing transfer of microbial biomolecules by outer membrane vesicles in microbe-host-communication in vivo. *Journal of Extracellular Vesicles*, *10*(12), e12159. https://doi.org/10.1002/jev2.12159

Bolam, D. N., & van den Berg, B. (2018). TonB-dependent transport by the gut microbiota: Novel aspects of an old problem. *Current Opinion in Structural Biology*, *51*, 35–43.

Bui, F. Q., Almeida-da-Silva, C. L. C., Huynh, B., Trinh, A., Liu, J., Woodward, J., Asadi, H., & Ojcius, D. M. (2019). Association between periodontal pathogens and systemic disease. *Biomedical Journal*, *42*(1), 27–35. https://doi.org/10.1016/j.bj.2018.12.001

Caruana, J. C., & Walper, S. A. (2020). Bacterial membrane vesicles as mediators of microbe—microbe and microbe—host community interactions. *Frontiers in Microbiology*, *11*, 432.

Cecil, J. D., O'Brien-Simpson, N. M., Lenzo, J. C., Holden, J. A., Chen, Y. Y., Singleton, W., Gause, K. T., Yan, Y., Caruso, F., & Reynolds, E. C. (2016). Differential responses of pattern recognition receptors to outer membrane vesicles of three periodontal pathogens. *PLoS ONE*, *11*(4), e0151967. https://doi.org/10.1371/journal.pone.0151967

Chen, G., Sun, Q., Cai, Q., & Zhou, H. (2022). Outer membrane vesicles from *Fusobacterium nucleatum* switch M0-like macrophages toward the M1 phenotype to destroy periodontal tissues in mice. *Frontiers in Microbiology*, *13*, 815638.

Chinthamani, S., Settem, R. P., Honma, K., Stafford, G. P., & Sharma, A. (2022). *Tannerella forsythia* strains differentially induce interferon gamma-induced protein 10 (IP-10) expression in macrophages due to lipopolysaccharide heterogeneity. *Pathogens and Disease*, *80*(1), ftac008.

Choi, D., Go, G., Kim, D. K., Lee, J., Park, S. M., Di Vizio, D., & Gho, Y. S. (2020). Quantitative proteomic analysis of trypsin-treated extracellular vesicles to identify the real-vesicular proteins. *Journal of Extracellular Vesicles*, *9*(1), 1757209. https://doi.org/10.1080/20013078.2020.1757209

Chukkapalli, S. S., Rivera-Kweh, M. F., Velsko, I. M., Chen, H., Zheng, D., Bhattacharyya, I., Gangula, P. R., Lucas, A. R., & Kesavalu, L. (2015). Chronic oral infection with major periodontal bacteria *Tannerella* forsythia modulates systemic atherosclerosis risk factors and inflammatory markers. *Pathogens and Disease*, *73*(3), ftv009. https://doi.org/10.1093/femspd/ftv009

Cox, J., & Mann, M. (2008). MaxQuant enables high peptide identification rates, individualized p.p.b.-range mass accuracies and proteome-wide protein quantification. *Nature Biotechnology*, *26*(12), 1367–1372.

Cox, J., Neuhauser, N., Michalski, A., Scheltema, R. A., Olsen, J. V., & Mann, M. (2011). Andromeda: A peptide search engine integrated into the MaxQuant environment. *Journal of Proteome Research*, *10*(4), 1794–1805. https://doi.org/10.1021/pr101065j

Dhondt, B., Lumen, N., De Wever, O., & Hendrix, A. (2020). Preparation of multi-omics grade extracellular vesicles by density-based fractionation of urine. *STAR Protocols*, *1*(2), 100073.

Elsayed, R., Elashiry, M., Liu, Y., El-Awady, A., Hamrick, M., & Cutler, C. W. (2021). *Porphyromonas gingivalis* provokes exosome secretion and paracrine immune senescence in bystander dendritic cells. *Frontiers in Cellular and Infection Microbiology*, *11*, 669989. https://doi.org/10.3389/fcimb.2021.669989

Fan, R., Zhou, Y., Chen, X., Zhong, X., He, F., Peng, W., Li, L., Wang, X., & Xu, Y. (2023). *Porphyromonas gingivalis* outer membrane vesicles promote apoptosis via msRNA-regulated DNA methylation in periodontitis. *Microbiology Spectrum*, *11*(1), e0328822. https://doi.org/10.1128/spectrum.03288-22

Fitzgerald, W., Freeman, M. L., Lederman, M. M., Vasilieva, E., Romero, R., & Margolis, L. (2018). A system of cytokines encapsulated in extracellular vesicles. *Scientific Reports*, *8*(1), 8973. https://doi.org/10.1038/s41598-018-27190-x

Friedrich, V., Gruber, C., Nimeth, I., Pabinger, S., Sekot, G., Posch, G., Altmann, F., Messner, P., Andrukhov, O., & Schäffer, C. (2015). Outer membrane vesicles of *Tannerella forsythia*: Biogenesis, composition, and virulence. *Molecular Oral Microbiology*, *30*(6), 451–473. https://doi.org/10.1111/omi.12104

Ge, S. X., Jung, D., & Yao, R. (2020). ShinyGO: A graphical gene-set enrichment tool for animals and plants. *Bioinformatics*, *36*(8), 2628–2629.

Gomes, F. I., Aragão, M. G., Barbosa, F. C., Bezerra, M. M., de Paulo Teixeira Pinto, V., & Chaves, H. V. (2016). Inflammatory cytokines interleukin-1β and tumour necrosis factor-α—Novel biomarkers for the detection of periodontal diseases: A literature review. *Journal of Oral & Maxillofacial Research*, *7*(2), e2. https://doi.org/10.5037/jomr.2016.7202

Graves, D. T., & Cochran, D. (2003). The contribution of interleukin-1 and tumor necrosis factor to periodontal tissue destruction. *Journal of Periodontology*, *74*(3), 391–401.

Hajishengallis, G. (2015). Periodontitis: From microbial immune subversion to systemic inflammation. *Nature Reviews: Immunology*, *15*(1), 30–44.

Jeppesen, D. K., Fenix, A. M., Franklin, J. L., Higginbotham, J. N., Zhang, Q., Zimmerman, L. J., Liebler, D. C., Ping, J., Liu, Q., Evans, R., Fissell, W. H., Patton, J. G., Rome, L. H., Burnette, D. T., & Coffey, R. J. (2019). Reassessment of exosome composition. *Cell*, *177*(2), 428–445.e18. https://doi.org/10.1016/j.cell.2019.02.029

Jun, H. K., Lee, S. H., Lee, H. R., & Choi, B. K. (2012). Integrin alpha5beta1 activates the NLRP3 inflammasome by direct interaction with a bacterial surface protein. *Immunity*, *36*(5), 755–768.

Jung, Y. J., Choi, Y. J., An, S. J., Lee, H. R., Jun, H. K., & Choi, B. K. (2017). *Tannerella forsythia* GroEL induces inflammatory bone resorption and synergizes with interleukin-17. *Molecular Oral Microbiology*, *32*(4), 301–313. https://doi.org/10.1111/omi.12172

Karn, V., Ahmed, S., Tsai, L. W., Dubey, R., Ojha, S., Singh, H. N., Kumar, M., Gupta, P. K., Sadhu, S., Jha, N. K., Kumar, A., Pandit, S., & Kumar, S. (2021). Extracellular vesicle-based therapy for COVID-19: Promises, challenges and future prospects. *Biomedicines*, *9*(10), 1373. https://doi.org/10.3390/biomedicines9101373

Kim, H. Y., Song, M. K., Gho, Y. S., Kim, H. H., & Choi, B. K. (2021). Extracellular vesicles derived from the periodontal pathogen *Filifactor alocis* induce systemic bone loss through Toll-like receptor 2. *Journal of Extracellular Vesicles*, *10*(12), e12157.

Kinane, D. F., Stathopoulou, P. G., & Papapanou, P. N. (2017). Periodontal diseases. *Nature Reviews Disease Primers*, *3*, 17038.

Ko, Y. K., An, S. J., Han, N. Y., Lee, H., & Choi, B. K. (2019). Regulation of IL-24 in human oral keratinocytes stimulated with *Tannerella forsythia*. *Molecular Oral Microbiology*, *34*(5), 209–218.

Kuipers, M. E., Hokke, C. H., & Smits, H. H., & Nolte-'t Hoen, E. N. M. (2018). Pathogen-derived extracellular vesicle-associated molecules that affect the host immune system: An overview. *Frontiers in Microbiology*, *9*, 2182.

Lekmeechai, S., Su, Y. C., Brant, M., Alvarado-Kristensson, M., Vallström, A., Obi, I., Arnqvist, A., & Riesbeck, K. (2018). *Helicobacter pylori* outer membrane vesicles protect the pathogen from reactive oxygen species of the respiratory burst. *Frontiers in Microbiology*, *9*, 1837. https://doi.org/10.3389/fmicb.2018.01837

Lim, Y., Kim, H. Y., An, S. J., & Choi, B. K. (2022). Activation of bone marrow-derived dendritic cells and $CD4^+$ T cell differentiation by outer membrane vesicles of periodontal pathogens. *Journal of Oral Microbiology*, *14*(1), 2123550.

Liu, Y., Defourny, K. A. Y., Smid, E. J., & Abee, T. (2018). Gram-positive bacterial extracellular vesicles and their impact on health and disease. *Frontiers in Microbiology*, *9*, 1502.

Luchian, I., Goriuc, A., Sandu, D., & Covasa, M. (2022). The role of matrix metalloproteinases (MMP-8, MMP-9, MMP-13) in periodontal and peri-implant pathological processes. *International Journal of Molecular Sciences*, *23*(3), 1806.

Macdonald, I. A., & Kuehn, M. J. (2013). Stress-induced outer membrane vesicle production by *Pseudomonas aeruginosa*. *Journal of Bacteriology*, *195*(13), 2971–2981.

Manning, A. J., & Kuehn, M. J. (2011). Contribution of bacterial outer membrane vesicles to innate bacterial defense. *BMC Microbiology*, *11*, 258.

Myneni, S. R., Settem, R. P., Sojar, H. T., Malone, J. P., Loimaranta, V., Nakajima, T., & Sharma, A. (2012). Identification of a unique TLR2-interacting peptide motif in a microbial leucine-rich repeat protein. *Biochemical and Biophysical Research Communications*, *423*(3), 577–582. https://doi.org/10.1016/j.bbrc.2012.06.008

Nara, P. L., Sindelar, D., Penn, M. S., Potempa, J., & Griffin, W. S. T. (2021). *Porphyromonas gingivalis* outer membrane vesicles as the major driver of and explanation for neuropathogenesis, the cholinergic hypothesis, iron dyshomeostasis, and salivary lactoferrin in Alzheimer's disease. *Journal of Alzheimer's Disease*, *82*(4), 1417–1450.

Nazir, M. A. (2017). Prevalence of periodontal disease, its association with systemic diseases and prevention. *International Journal of Health Sciences (Qassim)*, *11*(2), 72–80.

Noh, M. K., Jung, M., Kim, S. H., Lee, S. R., Park, K. H., Kim, D. H., Kim, H. H., & Park, Y. G. (2013). Assessment of IL-6, IL-8 and TNF-α levels in the gingival tissue of patients with periodontitis. *Experimental and Therapeutic Medicine*, *6*(3), 847–851. https://doi.org/10.3892/etm.2013.1222

Okamura, H., Hirota, K., Yoshida, K., Weng, Y., He, Y., Shiotsu, N., Ikegame, M., Uchida-Fukuhara, Y., Tanai, A., & Guo, J. (2021). Outer membrane vesicles of *Porphyromonas gingivalis*: Novel communication tool and strategy. *The Japanese Dental Science Review*, *57*, 138–146. https://doi.org/10.1016/j.jdsr.2021.07.003

Oliveira-Nascimento, L., Massari, P., & Wetzler, L. M. (2012). The role of TLR2 in infection and immunity. *Frontiers in Immunology*, *3*, 79.

Palomino, R. A. N., Vanpouille, C., Costantini, P. E., & Margolis, L. (2021). Microbiota-host communications: Bacterial extracellular vesicles as a common language. *PLoS Pathogens*, *17*(5), e1009508.

Perez-Riverol, Y., Bai, J., Bandla, C., García-Seisdedos, D., Hewapathirana, S., Kamatchinathan, S., Kundu, D. J., Prakash, A., Frericks-Zipper, A., Eisenacher, M., Walzer, M., Wang, S., Brazma, A., & Vizcaíno, J. A. (2022). The PRIDE database resources in 2022: a hub for mass spectrometry-based proteomics evidences. *Nucleic Acids Research*, *50*(D1), D543–D552. https://doi.org/10.1093/nar/gkab1038

Renkl, A. C., Wussler, J., Ahrens, T., Thoma, K., Kon, S., Uede, T., Martin, S. F., Simon, J. C., & Weiss, J. M. (2005). Osteopontin functionally activates dendritic cells and induces their differentiation toward a Th1-polarizing phenotype. *Blood*, *106*(3), 946–955. https://doi.org/10.1182/blood-2004-08-3228

Sahoo, S., Adamiak, M., Mathiyalagan, P., Kenneweg, F., Kafert-Kasting, S., & Thum, T. (2021). Therapeutic and diagnostic translation of extracellular vesicles in cardiovascular diseases: Roadmap to the clinic. *Circulation*, *143*(14), 1426–1449. https://doi.org/10.1161/CIRCULATIONAHA.120.049254

Schwechheimer, C., & Kuehn, M. J. (2015). Outer-membrane vesicles from Gram-negative bacteria: Biogenesis and functions. *Nature Reviews: Microbiology*, *13*(10), 605–619.

Shao, S., Fang, H., Li, Q., & Wang, G. (2020). Extracellular vesicles in inflammatory skin disorders: From pathophysiology to treatment. *Theranostics*, *10*(22), 9937–9955.

Sharma, A. (2010). Virulence mechanisms of *Tannerella forsythia*. *Periodontology 2000*, *54*(1), 106–116.

Shu, S., Yang, Y., Allen, C. L., Hurley, E., Tung, K. H., Minderman, H., Wu, Y., & Ernstoff, M. S. (2019). Purity and yield of melanoma exosomes are dependent on isolation method. *Journal of Extracellular Vesicles*, *9*(1), 1692401. https://doi.org/10.1080/20013078.2019.1692401

Suh, J., Han, D., Ku, J. H., Kim, H. H., Kwak, C., & Jeong, C. W. (2022). Next-generation proteomics-based discovery, verification, and validation of urine biomarkers for bladder cancer diagnosis. *Cancer Research and Treatment*, *54*(3), 882–893. https://doi.org/10.4143/crt.2021.642

Thery, C., Ostrowski, M., & Segura, E. (2009). Membrane vesicles as conveyors of immune responses. *Nature Reviews: Immunology*, *9*(8), 581–593.

Théry, C., Witwer, K. W., Aikawa, E., Alcaraz, M. J., Anderson, J. D., Andriantsitohaina, R., Antoniou, A., Arab, T., Archer, F., Atkin-Smith, G. K., Ayre, D. C., Bach, J. M., Bachurski, D., Baharvand, H., Balaj, L., Baldacchino, S., Bauer, N. N., Baxter, A. A., Bebawy, M., … Zuba-Surma, E. K. (2018). Minimal information for studies of extracellular vesicles 2018 (MISEV2018): A position statement of the International Society for Extracellular Vesicles and update of the MISEV2014 guidelines. *Journal of Extracellular Vesicles*, *7*(1), 1535750. https://doi.org/10.1080/20013078.2018.1535750

Thumuluri, V., Almagro Armenteros, J. J., Johansen, A. R., Nielsen, H., & Winther, O. (2022). DeepLoc 2.0: Multi-label subcellular localization prediction using protein language models. *Nucleic Acids Research*, *50*(W1), W228–W234.

Tyanova, S., Temu, T., Sinitcyn, P., Carlson, A., Hein, M. Y., Geiger, T., Mann, M., & Cox, J. (2016). The Perseus computational platform for comprehensive analysis of (prote)omics data. *Nature Methods*, *13*(9), 731–740. https://doi.org/10.1038/nmeth.3901

van de Waterbeemd, B., Zomer, G., van den Ijssel, J., van Keulen, L., Eppink, M. H., van der Ley, P., & van der Pol, L. A. (2013). Cysteine depletion causes oxidative stress and triggers outer membrane vesicle release by *Neisseria meningitidis*; implications for vaccine development. *PLoS ONE*, *8*(1), e54314. https://doi.org/10.1371/journal.pone.0054314

Veith, P. D., Chen, Y. Y., Chen, D., O'Brien-Simpson, N. M., Cecil, J. D., Holden, J. A., Lenzo, J. C., & Reynolds, E. C. (2015). *Tannerella forsythia* outer membrane vesicles are enriched with substrates of the Type IX secretion system and TonB-dependent receptors. *Journal of Proteome Research*, *14*(12), 5355–5366. https://doi.org/10.1021/acs.jproteome.5b00878

Villard, A., Boursier, J., & Andriantsitohaina, R. (2021). Microbiota-derived extracellular vesicles and metabolic syndrome. *Acta Physiologica (Oxford, England)*, *231*(4), e13600.

Yoo, H.-J., & Lee, S.-H. (2021). Heme effects of hemin on growth of peridontopathogens. *Journal of Dental Rehabilitation and Applied Science*, *37*(1), 31–38.

Yoo, J. Y., Kim, H. C., Zhu, W., Kim, S. M., Sabet, M., Handfield, M., Hillman, J., Progulske-Fox, A., & Lee, S. W. (2007). Identification of *Tannerella forsythia* antigens specifically expressed in patients with periodontal disease. *FEMS Microbiology Letters*, *275*(2), 344–352. https://doi.org/10.1111/j.1574-6968.2007.00906.x

Yost, S., & Duran-Pinedo, A. E. (2018). The contribution of *Tannerella forsythia* dipeptidyl aminopeptidase IV in the breakdown of collagen. *Molecular Oral Microbiology*, *33*(6), 407–419.

Yu, C. S., Cheng, C. W., Su, W. C., Chang, K. C., Huang, S. W., Hwang, J. K., & Lu, C. H. (2014). CELLO2GO: A web server for protein subCELlular LOcalization prediction with functional gene ontology annotation. *PLoS ONE*, *9*(6), e99368. https://doi.org/10.1371/journal.pone.0099368

Zhang, Z., Liu, D., Liu, S., Zhang, S., & Pan, Y. (2020). The role of *Porphyromonas gingivalis* outer membrane vesicles in periodontal disease and related systemic diseases. *Frontiers in Cellular and Infection Microbiology*, *10*, 585917.

SUPPORTING INFORMATION

Additional supporting information can be found online in the Supporting Information section at the end of this article.

How to cite this article: Lim, Y., Kim, H. Y., Han, D., & Choi, B.-K. (2023). Proteome and immune responses of extracellular vesicles derived from macrophages infected with the periodontal pathogen *Tannerella forsythia*. *Journal of Extracellular Vesicles*, *12,* e12381. https://doi.org/10.1002/jev2.12381